ELSEVIER

Avengers against cancer: A new era of nano-biomaterial-based therapeutics

Nishant Kumar, Sajid Fazal, Eijiro Miyako *, Kazuaki Matsumura *, Robin Rajan *

School of Materials Science, Japan Advanced Institute of Science and Technology, 1-1 Asahidai, Nomi, Ishikawa 923-1292, Japan

Cancer is one of the leading causes of death worldwide. As the cancer burden continues to increase globally, it exerts tremendous physical, emotional, and financial strain on individuals, families, communities, and health care systems. Cancer can affect any part of the body and is characterized by its uncontrollable growth. Numerous treatments, such as radiation therapy and chemotherapy which utilize various drugs, are currently in use; however, their harmful side effects and the development of drug resistance have resulted in major roadblocks when treating cancer. With advancements in synthetic and polymer chemistry, the use of nanoparticle-based drug delivery systems and chemotherapeutic macromolecules have garnered increasing attention in the previous decade. This review discusses the recent advancements in the use of nanoparticle-based drug delivery systems as well as the development of synthetic biodegradable polypeptides and polymers for cancer treatment (both *in vivo* and *in vitro*). Additionally, we outline the potent selectivity and efficacy for immunotherapies and bacteria-based therapies that are used to treat various cancers.

Keywords: Nanomedicine; Drug delivery; Polypeptides; Cationic polymers; Bacteria therapy; Immunotherapy

Introduction

The word cancer is used to define a large group of heterogeneous diseases that are characterized by uncontrollable cellular growth. It can originate in any body part, including organs or tissues, and has the potential to invade and spread throughout the body. Genetic alterations, such as mutations in DNA repair genes, oncogenes, tumor suppressor genes, as well as other genes involved in cellular growth and differentiation, transform normal cells into malignant cancer cells. Cancer is one of the major causes of mortality/morbidity worldwide, ranking second after cardiovascular diseases. According to the WHO, in 2020 it accounted for one in six deaths; estimations point to the occurrence of 9.9 million deaths and 1.9 million new cases (Fig. 1). The most common cancer types are breast, lung, cervical, colorectal, and thyroid, however, cancers of the mouth, liver, lung, stomach, prostate, and colon are more common in men [1].

Cancer cells differ from normal cells in various ways, such as their membrane compositions, energy consumption, and rate of proliferation. For instance, in normal eukaryotic cells, phosphatidylethanolamine and phosphatidylserine are present in the inner leaflet of the cell membrane, whereas choline-containing phospholipids, sphingomyelin, and phosphatidylcholine are mainly present in the outer leaflet. However, this array can be altered in response to a variety of internal and external stimuli that result in certain biological responses. In addition to phosphatidylserine, O-glycosylated mucins [2,3], sialylated gangliosides [4], and heparan sulfates [5] are also overexpressed

Abbreviations: CT, Computed tomography; MRI, magnetic resonance imaging; PET, positron emission tomography; IMRT, intensity-modulated radiotherapy; IGRT, image-guided radiotherapy; 3DCRT, 3D conformal radiotherapy; SBRT, stereotactic body radiation therapy; EPR, enhanced permeability and retention; PLGA, poly(lactic-co-glycolic acid); PLA, poly(lactide acid); PCL, poly (ε-caprolactone); PEG, poly(ethylene glycol); PVA, polyvinyl alcohol; PVP, poly (N-vinylpyrrolidone); CNHs, carbon nanohorns; NDs, nanodiamonds; PEI, polyethyleneimine; TRPV2, transient receptor potential vanilloid family type 2; ICG, indocyanine green; EGaIn, eutectic gallium-indium; Galinstan, gallium-indium-tin; TME, tumor microenvironment; PTT, photothermal therapy.

* Corresponding authors.

E-mail addresses: Miyako, E. (e-miyako@jaist.ac.jp), Matsumura, K. (mkazuaki@jaist.ac.jp), Rajan, R. (robin@jaist.ac.jp).

https://doi.org/10.1016/j.mattod.2021.09.020

in cancer cell membranes, whereas normal cell membranes are mainly composed of neutral zwitterionic phospholipids and sterols [6] (Fig. 2a). In tumor cells, a relatively higher number of microvilli are present in comparison to normal cells, thus increasing the surface area of the cancerous cells and allowing them to interact with more cationic anticancer peptides and polymers [7]. Otto Warburg proposed that the consumption of energy in cancer cells is different from that in normal cells [8]. Cancer cells do not perform the tricarboxylic acid (TCA) cycle for energy production; as they prefer the glycolytic pathway, even in the absence of oxygen, and thus have higher levels of lactate production which leads to acidification [9] (Fig. 2b) [10].

Globally, various methods are used to treat cancer, including radiation therapy, chemotherapy, and biomaterial-based drug treatments; in addition, various surgical procedures have also been utilized. Most treatment options have been extensively reviewed [11–14]. However, an exhaustive and detailed review focusing on the various aspects of biomaterial-based cancer treatments, including bacteria-based therapies, has not, to the best of our knowledge, been published prior to this review. Additionally, cationic polymers have recently been recognized as efficient alternatives to small molecule anticancer drugs, as they offer greater tunability and control over molecular structures and functions. There have been several exciting studies in the previous decade related to this topic that are also discussed in detail in this review.

In this review, we focus on the recent advances in cancer treatments and discuss the various aspects and strategies for overcoming the problems associated with tumor treatment and resistance. A detailed discussion of the various anticancer drug delivery systems, including stimuli-responsive systems and inorganic nanoparticles, and their advantages and limitations has been provided. Furthermore, we emphasize the development of macromolecules (polymers), polypeptides, and nanoparticles for use in cancer treatments, both *in vitro* and *in vivo,* and we discuss the selective mechanisms of different bioactive macromolecular pharmacophoric moieties on cancerous cells. With the known limitations of small-molecule drugs and conventional drug delivery systems, the potential use of polymeric molecules as anticancer agents could be a game-changer in the field of polymer-based biopharmaceuticals.

Cancer treatment

Historic perspective

The term cancer derives from the Greek word “karkinos”, which was first used to describe malignant tumors by the physician Hippocrates. Some of the earliest evidence of human bone cancer can be found in ancient Egyptian mummies and manuscripts (around 1600 BC). In medicine, the earliest written evidence of cancer (breast cancer), describes it as a grave disease with no treatment, and it was found in an ancient Egyptian medical text (Edwin Smith Papyrus) [15]. Examples of the treatments used by the Egyptians include cautery, surgery with knives, salts, and an arsenic paste that remained in use and was referred to as an “Egyptian ointment” until the 19th century [16]. In contrast, herbal remedies such as tea, figs, fruit juices, and boiled cabbage were used by the Sumerians, Indians, Chinese, and Persians; however, in severe cases, they would also use pastes of copper, iron, sulfur, and mercury. Some of these mixtures have been used on internal and external cancers for approximately 3000 years. Claudius Galen, a Greek medical practitioner, wrote more than 100 notes on tumors and cancer, which were translated from Greek to Latin and other languages and distributed globally at the time [17].

Conventional methods for cancer treatment

Today, surgery is often the first-line of treatment for malignant and solid tumors. After the discovery of anesthesia in 1846, surgeons such as Billroth, Handley, and Halsted performed the first tumor resections, as they removed entire tumors along with the lymph nodes. Different types of surgery are used for the treatment of cancer at different stages such as radical or curative surgery (removal of the entire tumor), surgery for symptomatic relief, conserving surgery, surgery for metastases, recurrent surgery, and reconstructive surgery. With advancements in technology, different surgical strategies have been developed, which can eliminate the need to cut with a scalpel. Since surgical methods involve pain, with the possibility of infection and death, and tend to be expensive, researchers have tried to develop less invasive, painful, and harmful alternative strategies to combat cancer, which are briefly reviewed in the following paragraphs.

Radiation therapy exposes cancer cells to high doses of radiation. The radiation does not directly kill the cancer cells but dam-

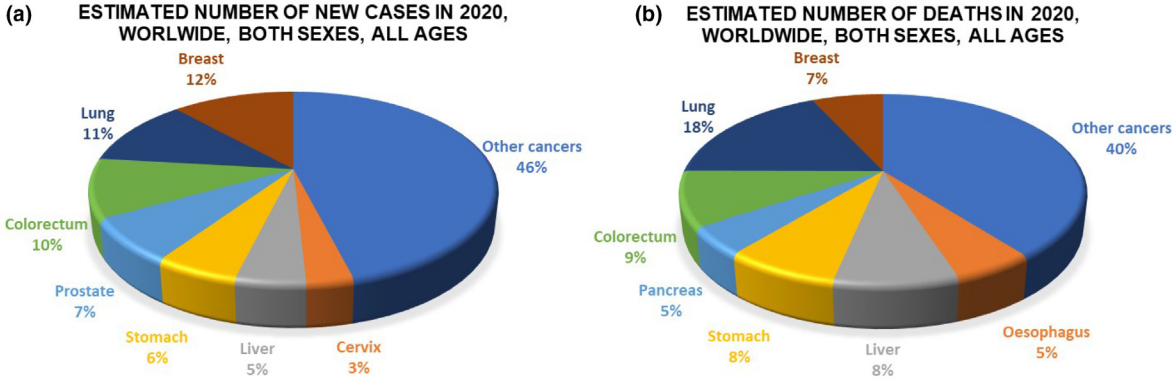

FIGURE 1

Global cancer burden in 2020. (a) Estimated new cases of cancer in 2020. (b) Estimated deaths due to cancer in 2020 [1].

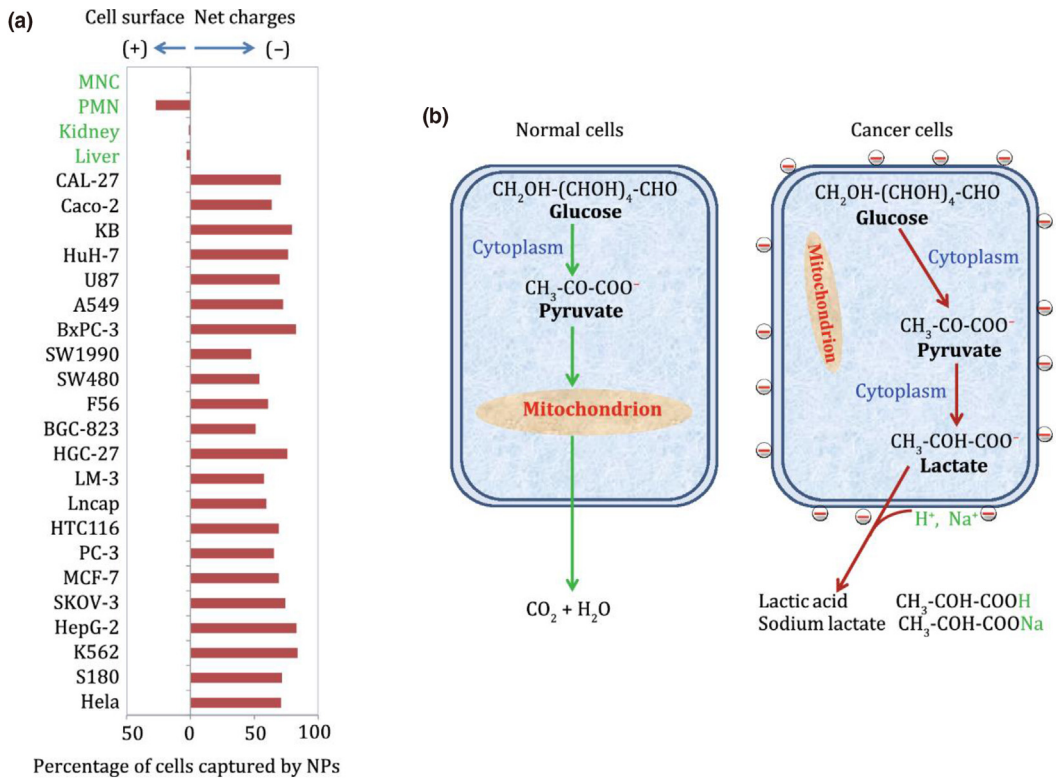

FIGURE 2

Differences in the membranes of cancer and normal cells. (a) The calculated net surface charges for various cell lines. (b) Diagram showing the production of lactate, which results in a more acidic environment and a negative charge on cancer cells. Reproduced with permission from Chen et al. [10], under the creative commons attribution (CC BY-NC) license.

ages the DNA beyond repair; as a result, the cells stop dividing, and die within weeks or months, and are consequently removed from the body. Radiation treatments depend on the type of cancer, size of the tumor(s), implications on the lymph nodes, and the type of radiation technique used [18]. Although improved imaging techniques and delivery methods have somewhat lowered the toxicity to nearby cells, further research is warranted to minimize the toxicity and side effects. Moreover, an understanding of the biological mechanisms is still required.

Chemotherapy involves the use of drugs systemically, to either stop or slow cancer cell growth. Based on the mode of action, the following classes of anticancer drugs are available: a) DNA damaging alkylating agents; b) RNA and DNA building block replacement anti-metabolites; c) DNA replication interfering antibiotics; d) topoisomerase I or II (enzymes involved in DNA replication and transcription) inhibitors; e) mitosis and cell division inhibitors; and f) corticosteroids [13]. Although chemotherapy shows good results for cancer treatment, it is not enough alone to eradicate the disease in most patients. Moreover, chemotherapy is also associated with severe side effects, immediate harmful effects on the hair, skin, blood, kidneys, and gastrointestinal tract, and the prolonged consequences of chemotherapy include drug resistance, carcinogenicity, and infertility [19].

Due to these known limitations and to lessen the death and pain caused by cancers, novel potential treatment methods are required. Gene therapy is a promising new method for the treatment of cancer. It involves the use of specific genetic material to modify cells (either *in vitro* or *in vivo*) for the treatment of various disorders [20]. For the treatment of cancer several approaches like anti-angiogenic gene therapy, immunotherapy, siRNA therapy, suicide gene therapy, and pro-apoptotic gene therapy have been developed [21]. Gene therapy has already been successfully used to treat various kinds of cancer [22–24], and a detailed discussion of this can be found in the review by Giamas [25].

Material-based treatments

While the methods discussed in the preceding section have yielded impressive results, they also suffer from many drawbacks. As the prevalence of cancer is increasing each year, it is imperative that we develop new therapeutic materials to manage and treat it. Accordingly, over the years, many material-based cancer therapeutics have been developed. Material-based methods offer greater flexibility and potency when compared to conventional methods, and hence have gained widespread popularity in previous decades. In the following sections, we have broadly classified material-based therapeutic methods into two categories: materials used to deliver anticancer drugs such as drug delivery systems, and materials which can be directly used to treat cancer without the need for any additional cargo. We also discuss the various subcategories and modes of action for these molecules when treating cancer.

Materials as drug-delivery systems

Nanoparticles as cancer therapeutics

Although surgical resection, radiation therapy, and chemotherapy have achieved success in the treatment of cancer, better therapeutic strategies that improve overall survival, reduce treatment side effects, increase patient compliance, and improve disease management and outcomes are sought-after in clinics. To achieve this, it is imperative that we develop a rational treatment strategy that combines and maximizes both efficacy and safety to not only treat the disease effectively but also maintain patient welfare. Nanotechnology-based treatment options, which allow for the combination of different treatment modalities, drugs, and materials in one single platform, have thus become extremely attractive. For instance, the loading of drugs into nanoparticles alters the pharmacokinetic properties of the drugs [26] (e.g., improved biodistribution, greater bioavailability, and lower clearance), prevents their degradation inside the body, and reduces drug toxicity and side effects [27]; the nanoparticles carrying the drugs interact primarily with the surrounding biological environment through their surface functional groups [28], which ultimately dictates the fate of the drug. In fact, the high surface-area-to-volume ratio of the nanoparticles is an advantage because of the subtle changes in surface functionality which can enable drastic changes in their properties inside the body. Additionally, the small size of nanoparticles (10–500 nm) provides unique advantages over the free drug molecules. This is because the enhanced permeability and retention (EPR) effects that are found in many tumors enable nanoparticle accumulation/retention at the tumor site, which is difficult to achieve when using small sized free drugs [29]. Moreover, the nanoparticle surface area can be appropriately modified to incorporate ligands targeting tumor sites without compromising the functional ability of the loaded drug. Importantly, the biggest advantage of nanoparticles in drug delivery is their ability to incorporate materials with different functionalities. "Multi-functional" nanoparticle systems can be designed via the loading of multiple drugs to increase the overall therapeutic efficacy; additionally, stimuli-responsive materials for remote-controlled on-demand drug release, together with diagnostic and therapeutic components for image-guided drug delivery can also be incorporated. Broadly, nanoparticles for drug delivery applications can be classified based on the material used to synthesize them: polymer-based nanoparticles, lipid-based nanoparticles, non-polymeric nanoparticles, and nanoparticles derived from biological materials (Fig. 3). These different systems are briefly discussed below.

Polymer-based nanoparticles. Nanoparticles made from polymeric materials are usually considered suitable for drug delivery applications because their physicochemical properties can be easily controlled (the chemical functionality of the polymer building blocks can be altered, as can be the reaction chemistry used for the synthesis of polymeric nanoparticles). Of note, for drug delivery applications, it is essential that nanoparticles can facilitate controlled drug release at the target site, without toxic effects. A few different types of artificial and natural polymers have been utilized for this purpose (Table 1).

Polymer nanoparticles. To synthesize nanoparticles from artificial polymers for drug delivery applications, FDA-approved polymers, are widely utilized, including poly(lactic-co-glycolic acid) (PLGA), poly(lactide acid) (PLA), poly(ε-caprolactone) (PCL), poly(ethylene glycol) (PEG), polyvinyl alcohol (PVA), and poly (N-vinylpyrrolidone) (PVP), as they are non-toxic, biocompatible, and biodegradable. To control the rate of degradation and eventual drug release, several different parameters can be optimized, including the molecular weight, end-group functionality, and nanoparticle size. For example, for PLGA nanoparticles, decreasing the ratio of lactide to glycolide increases their hydrophilicity and rate of degradation, and consequently drug release [56]. Other external factors such as the pH and temperature can also affect the drug release rate, and they can thus be modulated for the development of stimuli-responsive drug delivery systems. Studies have also shown how a copolymer (or two different polymers) can be used to load both hydrophobic and hydrophilic drugs together in a single system [57]. Core-shell polymeric nano-architectures have also been synthesized, showing unique drug protection and release rate kinetics in a biological environment [58]. Apart from the conventional FDA approved polymers mentioned above, new polymeric materials such as poly-N-(2-hydroxypropyl) methacrylamide [poly (HPMA)] [59,60] and polyoxazoline [61] have also shown promise as biocompatible drug delivery systems. Additionally, it should be noted that at present most polymeric drug delivery systems under investigation have stimuli-responsive properties (discussed later), which are known to significantly improve the therapeutic outcomes.

Dendrimers. Dendrimers are nanosized hyperbranched polymeric structures that have gained importance in the field of nanomedicine, especially for drug delivery. Their unique hyperbranched structures (Fig. 4a) and the corresponding high density of their surface functional groups gives them unique properties, unlike other nanomedical systems. Typically, dendrimers are composed of an inner core, branching layers, and a multivalent outer shell [62]. Since the branching layers are hydrophobic in nature, hydrophobic drugs can be attached to dendrimers within this layer, to increase their solubility under physiological conditions, and consequently to ensure effectiveness. For example, hydrophobic cargo such as phthalocyanines [63] and camptothecins [64] are encapsulated within dendrimers to increase their solubility in aqueous environments. On the other hand, drug molecules can also be attached to the dendrimer surface either through complexation or through different conjugation routes (methotrexate [65], doxorubicin [66], and paclitaxel [67]) depending on the available surface functional groups. Of note, dendrimers have cationic, anionic, and neutral surface functional groups that have been used for various applications, including tissue engineering [68], transfection [69], and antibacterial therapy [70], as well as drug delivery. However, concerns regarding the toxicity of positively charged cationic dendrimers has been reported in the literature, which warrants further investigation of their use *in vivo* [62].

Polymeric micelles. Polymeric micelles are nanosized structures with a hydrophobic core and a hydrophilic surface, that are formed by the self-assembly of amphiphilic block copolymers in an aqueous environment (Fig. 4b). In organic solvents, micelles with opposite orientations can also be formed, these have a hydrophilic core and a hydrophobic surface and are also called reverse micelles.

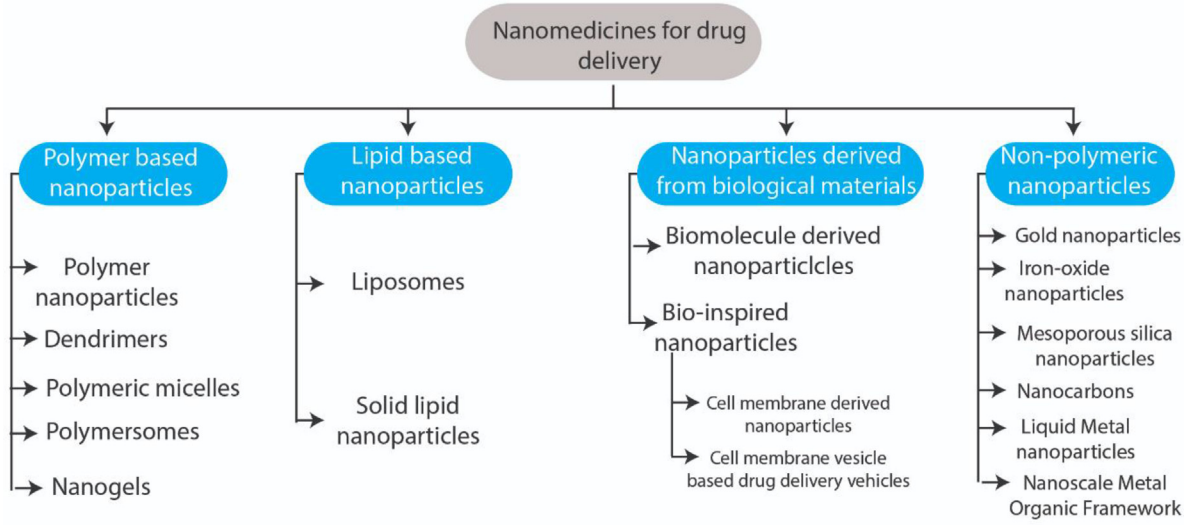

FIGURE 3

Classification of nanoparticles for drug delivery based on the materials used for their synthesis.

The self-assembly of amphiphilic copolymers into micellar structures occurs when the concentrations of the polymers in the aqueous medium increase beyond a concentration called the critical micelle concentration (CMC) [71]. Above this concentration, the formed micelles are in thermodynamic equilibrium with the free polymers in solution. For practical applications, the designed polymers should have a low critical micelle concentration such that the micelle structures remain stable at low concentrations when injected inside the body [72]. Both micelles and reverse micelles have been utilized in drug delivery applications [73]. The most widely used hydrophilic component in the micelles is PEG, as it can impart favorable pharmacokinetic properties to the delivery vehicle and prevent the uptake and clearance of drugs by macrophages [74]. Other polymers that have been reported to form hydrophilic components include PVP [75], poly(N-isopropyl acrylamide) (pNIPAM) [76], poly(trimethylene carbonate) [77], and poly(acryloylmorpholine) [78]. Of note, the hydrophobic component of the micelles can be composed of either polymers or lipids. Importantly, the choice of hydrophobic component and its interactions with the loaded drug play a key role in the drug-loading capacity of the synthesized micelles. Compared to other nanoparticulate structures, micelles [owing to their small size (<100 nm)] are considered effective for tumor therapy, as they can penetrate the leaky tumor vasculature and deliver drugs at high concentrations to the tumor site [79]. Kataoka and his team have published a series of reports using polymeric micelle-based drug delivery systems [80,81], including polypeptide based-micelles such as poly(ethylene glycol)-poly (aspartic acid) [82], and cyclic RGD-linked micelles made of poly(ethylene glycol)-b-poly-(L-glutamic acid) [83]; the loading of different anticancer agents showed remarkable targeting and efficacy. Remarkably, a number of different polymeric micelle formulations are currently undergoing clinical trials and are at various stages (docetaxel micelles for ovarian cancer, NCT03742713; paclitaxel micelles for breast cancer, NCT01644890; and oxaliplatin micelles for lymphomas, NCT01999491) [84].

Simple self-assembled micelles when used for drug-delivery applications may possess a major disadvantage with regards to their stability when used in-vivo. This is because after injection, when they are diluted in large volumes of blood, their thermodynamic equilibrium state ceases, causing them to dissociate and prematurely release the loaded drug into the body. To improve polymeric micelle stability, chemical cross-linking of the micelle shell or core is routinely employed [85]. Additionally, the covalent conjugation of the hydrophobic drug molecules to the micelle core is also utilized to improve micelle-drug interactions and stability [86]. Such micelles are rationally designed to incorporate cleavable cross-linkers which can facilitate a stimuli-responsive preferential drug release at the tumor site (discussed later).

Polymeric vesicles/polymersomes. Similar to liposomes, polymersomes are also comprised of a vesicle structure which is bound by a membrane; however, their membranes are composed of amphiphilic polymers. Due to the inherent flexibility that polymers provide in-terms of the choice of their chemical composition, degree of polymerization, and the versatility in the arrangement of hydrophilic and hydrophobic polymeric blocks, polymersomes could be considered superior to liposomes in terms of their chemical functionality. For example, the amphiphilic polymers used for synthesizing polymersomes can have compositions that deviate from the typical A-B (A- hydrophilic, B- hydrophobic) block co-polymer structure to A-B-A, A-B-C compositions, which can form polymersomes with slightly different membrane dynamics while still maintaining their vesicular nature. Importantly, since the stability of these vesicular structures (polymersomes or liposomes) is dependent on the inter/intra-chain hydrophobic interactions, the use of polymers composed of much longer hydrophobic blocks can be an advantage when compared to liposomes. Due to this difference, polymersomes can form vesicles with thicker membranes (~50 nm) [87] which consequently have an enhanced structural stability and cargo retention. The loading of drug/cargo into polymersomes can be done through passive

TABLE 1

Different types of polymer- and lipid-based nanoparticles.

	Loaded cargo	Cancer type	Remarks	Reference
Polymer NPs	siRNA	Prostate (*in vitro* – LnCaP, PC3, DU145)	The PRINT method enables a high encapsulation efficiency for cargo	[30]
	Paclitaxel	Brain (*in vivo* -C6 glioma; dose: 5 mg/Kg)		[31]
	Paclitaxel and IR780 dye	Ovarian (*in vivo* – ST30; dose: 7 mg/Kg)	Near-infrared (NIR) light-induced drug release	[32]
	KRAS-siRNA	Pancreas (*in vivo* – KPPC-1)	Successful KRAS knockdown was observed	[33]
	Doxorubicin	Brain (*in vivo* - glioblastoma 101/8; dose: 2.5 mg/Kg)		[34]
Dendrimers	mi-RNA and doxorubicin	Breast (*in vitro*- MDA-MB-231)		[35]
	AZD4320 (Bcl-2/Bcl-xL inhibitor)	Blood (*in vivo* – RS4 lymphoblastic leukemia)		[36]
	Doxorubicin	Breast (*in vivo* – Walker 256; dose: 2 mg/Kg)	Reduces non-specific uptake in major organs	[37]
	siRNA targeting Hsp27	Prostate (*in vivo* – PC-3; dose: 0.25 mg/Kg)	Targets amphiphilic dendrimers showing efficient gene silencing	[38]
Micelles	Doxorubicin	Breast (*in vivo* – 4 T1; dose: 10 mg/Kg)	Improves drug pharmacokinetics and tumor-specific accumulation	[39]
	Curcumin	Cervical (*in vivo* – HeLa; dose: 10 mg/Kg)	Cross-linked micelles show enhanced tumor accumulation	[40]
	Doxorubicin	Breast (*in vivo* – 4 T1; dose: 20 mg/Kg)	Reversible cross-linked micelles used	[41]
	Docetaxel	Breast (*in vivo* – 4 T1; dose: 10 mg/Kg)	Therapeutic efficacy against breast cancer metastasis	[42]
Polymerosome	Docetaxel	Breast (*in vivo* −4T1, dose: 10 mg/Kg)	Folic acid conjugated NPs for tumor targeting	[43]
	Indocyanine green and doxorubicin	Breast (*in vivo* −4T1, dose: 10 mg/Kg)	Combined photothermal and drug delivery	[44]
	Iron oxide NPs and doxorubicin	Cervical (*in vitro* -HeLa)	Higher MR contrast obtained relative to IO NPs alone	[45]
	Doxorubicin	Cervical (*in vitro* -HeLa)	pH responsive drug release	[46]
Nanogels	Doxorubicin	Cervical (*in vitro* -HeLa)	Polymersome membrane cross-linked to form hollow-nanogels	[47]
	HSP-90 inhibitor (17-AAG), doxorubicin	Breast (*in vivo* - BT-474, dose: 6 mg/Kg)	Synergistic chemotherapy	[48]
	Nile red, Paclitaxel, Doxorubicin	Breast (*in vitro* -MCF-7)	Hydrophobic and hydrophilic drugs loaded	[49]
	Doxorubicin	Bone (*in vitro* -CAL-72)	Simple synthesis process using alginate biopolymer	[50]
Liposomes	Doxorubicin	Colon (*in vivo* -C26; dose: 10 mg/Kg)	Anti-angiogenesis therapy achieved by targeting with Arg-Gly-Asp (RGD) peptides	[51]
	5-Fluorouracil and doxorubicin	Breast (*in vivo* – 4 T1; dose: 3 mg/Kg doxorubicin and 0.62 mg/Kg 5-Fluorouracil)	Synergistic delivery of drugs achieves effective tumor therapy at low toxicity	[52]
Solid lipid NPs	Didoceylmethotrexate (ddMTX), a lipophilic prodrug form of methotrexate	Brain (*in vivo* – F98 glioma; dose: 1.6 mg/Kg)		[53]
	Paclitaxel	Lung (*in vivo* – M109; dose: 1 mg/Kg)	Effective tumor therapy achieved through the pulmonary route, reducing systemic toxicity	[54]
	Paclitaxel	Lung and breast (*in vivo* – H1975, H1650, H520, PC9, SK-BR-3; dose: 22 mg/Kg)		[55]

NPs, nanoparticles; PRINT, particle replication in non-wetting templates.

loading strategies where the hydrophobic or hydrophilic cargo can be dissolved either in the organic or aqueous solvent during their synthesis. In one such study, the drug doxorubicin was loaded into polymersomes (with hydrophilic poly (ethylene oxide) and hydrophobic block-poly(2-(diethylamino) ethyl methacrylate)-stat-poly(methoxyethyl methacrylate) blocks) by dissolving the drug in the aqueous phase [88]. Here, the choice of the hydrophilic block was made to impart a stimuli-responsive property to both ultrasound and low pH (discussed later) to trigger drug release remotely. While the poly(2-(diethylamino) ethyl methacrylate cationic group was introduced for lysosome destabilization and endosomal release. Upon its use in-vivo for the treatment of mice with HeLa tumors (at 2 mg/Kg doxorubicin dose), significant reductions in tumor volumes were obtained for the ultrasound exposed tumors when compared to the unexposed and free-drug treated controls. This and other

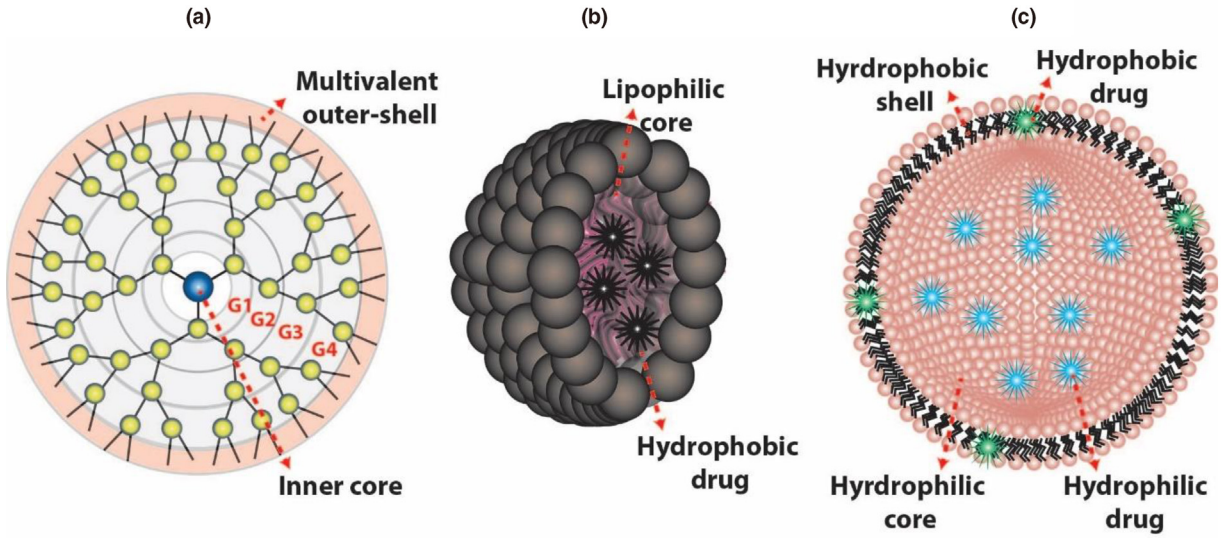

FIGURE 4

Structures of different polymer-based nanoparticles used as delivery systems. (a) Dendrimers, (b) micelles, and (c) liposomes.

research [89] has shown how tuning the chemical functionality of polymer building blocks when developing polymersomes allows for the incorporation of different treatment strategies in one platform. In another recent paper [89], the use of polymersomes for anti-cancer immunotherapy was demonstrated wherein the cargo (cGAMP- cyclic guanosine monophosphate–adenosine monophosphate; used for generating an anti-tumor immune response) was also loaded into polymersomes using simple passive loading during the synthesis procedure. Only a few studies however, have reported on the active loading of cargo using a pH gradient strategy (widely used for liposome loading) [90,91], or by the direct conjugation of the drug to the polymer building block [45]. While polymersomes display great flexibility in terms of their chemical functionality and membrane rigidity, there is inadequate information available to show their advantage over liposomal drug formulations when it comes to their practical applications [90].

Polymer nanogels. Nanogels are simply hydrogels that have nano-scaled dimensions. Similar to the general framework for hydrogel formation, which involves the chemical or physical cross-linking of hydrophilic polymers to form a three-dimensional gel network, nanogels are formed by physically limiting the volume of this cross-linking reaction in nano-scale dimensions. The process of creating a physically limited nano-sized reaction volume can be achieved through different techniques such as inverse mini-emulsions, microfluidics, inverse nanoprecipitation [92], and micellization [93], within which cross-linking reactions can be performed. The biggest advantage that nanogels confer when used as a drug delivery vehicle is that the three-dimensional porous hydrophilic polymeric network can act as a suitable cargo chamber which can protect it from external environmental factors such as heat, temperature, pH, and enzymes. Despite their hydrophilic cores, nanogels can be utilized as versatile drug carriers to load both hydrophilic and hydrophobic drugs [49,93]. In one such report, the hydrophobic fluorescent dye indocyanine green was loaded into hydrogels made of hyaluronic acid which were demonstrated to be successful for the imaging of MDA-MB-231 tumors in mice [94]. Moreover, a significant improvement of the pharmacokinetic properties of the loaded fluorescent dye could also be achieved with the intravenous administration of the nanogels. Similar to hydrogels, nanogels also inherently show stimuli-responsive behaviors which can be used for actuating remote-controlled drug release at the tumor site. To capitalize on this phenomenon, one such study reported the use of nanogels made from poly (methacrylic acid) loaded with doxorubicin for dual stimuli-responsive drug release [95]. An improved drug release profile was obtained when these nanogels were exposed to a lower pH and higher glutathione (GSH) concentrations (observed in many tumors environments-discussed later). The use of nanogels has also been explored for various other bio-medical applications such as vaccine delivery [96], tissue engineering [97], and enzyme stabilization [98], which further warrants its potential as a promising biomaterial in the future.

Lipid-based nanoparticles. Nanoparticles fabricated using lipids as building blocks can be largely classified into liposomes and solid lipid nanoparticles (Table 1).

Liposomes. Liposomes are composed of amphiphilic lipid molecules that contain a bulky hydrophobic group (e.g., glycolipids and phospholipids) and spontaneously rearrange when placed in an aqueous environment to form a vesicle-type structure with an inner hydrophilic core and an outer hydrophobic lipid bilayer shell (Fig. 4c). Due to their unique organization, liposomes can be used for the delivery of drugs with varying aqueous solubility degrees, both within the core and in the shell. Since liposomes are usually composed of naturally occurring lipids, they are highly biocompatible and non-immunogenic and can easily degrade in the body without producing any toxic effects. Therefore, it is not surprising that liposomes were the first class of nanoparticles approved by the FDA for cancer therapeutic applications [99]. FDA- and EMA-approved liposomal formulations [100] for the treatment of cancer include Doxil® [99] (ovarian

cancer), DaunoXome® [101] (Kaposi's sarcoma), Myocet™ [102] (metastatic breast cancer), Marqibo® [103] (acute lymphoblastic leukemia), MEPACT® [104] (osteosarcoma), and Onivyde® [105] (metastatic pancreatic cancer). However, all the clinically approved liposome formulations for cancer therapies to date are only passively targeted [106], even though ligand-functionalized actively targeted liposomes showed better effects pre-clinically. For example, liposomes functionalized with PEGylated transferrin have been demonstrated to deliver drugs across the blood–brain barrier [107] to transferrin receptor-overexpressing glioma cells in rats [108]. Similarly, studies have also demonstrated the functionalization of liposomes with anti-epidermal growth factor receptor [109] and anti-estrogen receptor [110] antibodies for targeted delivery to the tumor cells. In some reports, the dual functionalization of liposomes has also been carried out (for example, with both transferrin and arginine–glycine-aspartic acid-containing peptides [111]) to further enhance their targeting efficiency and drug delivery. Unlike other solid nanoparticles, the functionalization of liposomes with targeting ligands can be advantageous because the fluid-like lipid bilayer structure provides more flexibility for the ligand to interact with the substrate efficiently [112]. Currently, a number of active-targeted liposomes are undergoing clinical trials at various stages [113].

Solid lipid nanoparticles. Solid lipid nanoparticles are composed of a lipid core and a stabilizing surfactant, and their nanostructures are similar to those of polymeric nanoparticles. Lipids (such as triglycerides, fatty acids, fatty alcohols, and waxes) that are used for the synthesis of solid lipid nanoparticles are generally regarded as safe by the FDA. These lipids have melting points above the normal body temperature such that the nanostructures retain their structural integrity when used for biomedical applications. The surfactants used are amphiphilic molecules such as phospholipids, esters, and polysorbates that can interact favorably with both the lipid core and the surrounding aqueous environment and stabilize the particles. Solid lipid nanoparticles can be synthesized via many different techniques such as solvent emulsification/evaporation, microemulsion, ultrasonication, and high-pressure homogenization; the latter can be utilized on an industrial scale. The ease of synthesis on a large scale along with controlled drug delivery and long-term physicochemical stability makes them viable alternatives to liposomes. The ability to form a solid lipid core, unlike the vesicular structures in liposomes, allows for a slow and sustained drug release. Essentially, the crystallinity of the lipid core dictates their drug loading and release profile because highly crystalline lipid structures often exclude drug molecules from their matrix. Thus, the synthesis procedure should be fine-tuned to minimize lipid-core crystallinity (to increase drug loading); which can be done by incorporating different types of lipids within the core. Solid lipid nanoparticles can be utilized for the delivery of both hydrophilic and hydrophobic drugs, and a number of literature reports have demonstrated their ability to treat various cancers including those in the lungs [54], breasts [114], liver [115], and brain [53].

Nanoparticles from biologically derived materials. The third class of nanoparticles reviewed here are synthesized using materials obtained from a biological source; thus, they are biodegradable without any long-term toxic effects in the body. Several types of these nanoparticles have recently been developed and they showed potential for use in drug delivery and cancer therapies.

Biomolecule derived nanoparticles. These nanoparticles can be obtained by the direct assembly of biomolecules (Table 2), such as proteins (albumin and casein), polysaccharides (starch) and nucleic acids. In one study, paclitaxel-loaded human serum albumin nanoparticles were prepared for the treatment of triple-negative breast cancer: the intramolecular disulfide bonds (using GSH) within the albumin were reduced followed by the addition of paclitaxel to facilitate intermolecular disulfide bonding at a later stage. These nanoparticles showed greater therapeutic efficacy than free drugs when administered in breast tumor mouse models [116]. Of note, albumin as a protein source for nanoparticle synthesis provides several advantages from a pharmaceutical perspective [117], and as such is one of the most studied materials for drug delivery applications. Apart from its high biocompatibility and hydrophilicity, albumin is the most abundant plasma protein synthesized by the liver and can be easily purified and obtained on a commercial scale. Additionally, albumin can also be sourced from bovine serum (which has 76% sequence identity to human serum albumin [118]) at a low cost (bovine serum albumin is widely accepted in the pharmaceutical industry). In fact, the FDA- and EMA-approved albumin-bound paclitaxel (Abraxane™) is used for the treatment of metastatic breast cancer in clinics. Similarly, ferritin has also been investigated for drug delivery applications [119]. In a previous study, heavy chain ferritin was utilized for the synthesis of doxorubicin-loaded zinc nanocage structures for the treatment of colon cancer in mice [120]; drug loading was carried out via the careful disassembly of ferritin (using urea) in the presence of doxorubicin followed by reassembly, leading to the entrapment of drug molecules within the protein structure. In fact, the intrinsic ability of the ferritin heavy chain to bind to transferrin receptors (overexpressed in many cancer cells), allows for specific drug delivery and subsequent therapeutic responses. Of note, the ferritin heavy chain was successfully expressed in *Escherichia coli*, and thus can be mass-produced, facilitating clinical translation.

Unlike the other nanostructures described in this review, the nanoarchitectures that are obtained using nucleic acids are fundamentally unique. Nucleic acid nanotechnology encompasses nanostructures that are composed either solely of nucleic acids formed due to the canonical Watson-Crick base pairing [127] and other non-canonical base pairing [128] or by the organization of nucleic acids on nanoparticle surface templates [129]. By the self-assembly of carefully designed nucleotide sequences, nucleic acid nanostructures (2D and 3D) of varying sizes and shapes, such as cubic, tetrahedral, octahedral, and other miscellaneous structures can be obtained with a high degree of precision and flexibility. These structures are formed fundamentally due to double cross overs (holliday junctions) between single stranded DNA strands which enables the positioning of DNA strands at different planes. These nanostructures have excited researchers in this field and several reports have investigated their capabilities in relation to drug delivery applications. In one such study, triangle shaped DNA origami structures were synthesized that were found to show preferential accumulation and retention in tumor tissues when compared to square and tube-shaped DNA

TABLE 2

Types of biomolecules utilized in the synthesis of nanoparticles for drug delivery applications.

Biomolecule building block	Loaded cargo	Cancer type	Remarks	Reference
Albumin	Paclitaxel and fenretinide	Brain (*in vivo*- U87MG human glioma; dose – 2 mg/Kg)	Self-assembly of albumin protein for NP formation	[121]
Human H-ferritin	Doxorubicin	Brain (*in vivo*- U87MG human glioma; dose: 1 mg/Kg)	Inherent capability to be specifically taken up by tumor cells	[122]
Casein	10-Hydroxycamptothecin	Brain (*in vivo* – C6 glioma; dose: 5 mg/Kg)	Menthol modification increases brain penetration	[123]
Hydroxyethyl starch	Hydroxychloroquine	Pancreas (*in vitro* – PC cells)		[124]
RNA	Paclitaxel	Breast (*in vivo*- MDA-MB-231; dose: 8 mg/Kg)	EGFR was bound to the nanostructures for active targeting	[125]
DNA	Thrombin enzyme	Breast (*in vivo*- MDA-MB-231; dose: 1.5 units/mouse)	Site-specific cargo delivery enabled with the use of fastener strands that recognize nucleolin	[126]

NP, nanoparticle.

origami [130]. Such nanostructures loaded with anti-cancer doxorubicin showed significant tumor volume reductions when used for the delivery of doxorubicin for the treatment of MDA-MB-231 breast tumors (4 mg/Kg doxorubicin) when compared to the free drug. Similarly, in another study actively targeted drug-loaded tubular shaped DNA nanostructures [131] were synthesized by introducing cancer-ligand conjugated DNA to the unpaired single-stranded sections of the nucleic acid nanostructures. Here, doxorubicin drug loading could be accomplished by the simple mixing of the drug with the nanostructures due to the inherent preferential binding of the drug to the guanine-cytosine base pairs [132]. Even though nucleic acid nanostructures provide a great deal of flexibility and versatility in their preparation, functionalization and drug loading, the synthesis of such structures presently suffers from cumbersome designs and low yield [133].

Bio-inspired/biomimetic nanoparticles. To develop an ideal drug delivery system that shows high biocompatibility, minimal toxicity, and good pharmacokinetic properties (biodistribution and circulation times), bio-inspired/ biomimetic nanoparticles have been generated. Such nanoparticles are derived directly from cells and show excellent capability and functionality as drug delivery vehicles. Fundamentally, two types of biomimetic nanoparticles can be considered: cell membrane-derived nanoparticles and membrane vesicles derived directly from cells (exosomes, bacterial membrane vesicles).

Cell-membrane derived nanoparticles. The main strategy employed for the synthesis of such biomimetic nanoparticles involves the surface coating of conventional drug delivery vehicles such as polymer and inorganic nanoparticles with cell membrane structures (Fig. 5). The rationale is to modify the surface chemical properties of the drug delivery vehicles to impart/mimic the surface properties of the parent cell from which the membrane is derived. By doing so, favorable host-material interactions and pharmacokinetic properties can be achieved, including low immunogenicity and toxicity, reduced reticuloendothelial system clearance, high circulation time, and good biodistribution. The cell sources from which membranes are usually extracted (Table 3) include erythrocytes, white blood cells, cancer cells, mesenchymal stem cells, platelets, and bacteria. Among these, erythrocyte cell membrane-coated nanoparticles have been widely investigated [134–136] primarily because of their surface protein compositions, which include proteins such as CD47 [137] ("self-recognition" protein preventing immunological clearance), CD59 [138] (inhibits the formation of the membrane attack complex), and other surface proteins that inhibit/regulate the complement activation pathway (decay-accelerating factor, membrane cofactor protein, homologous restriction protein etc.), thereby rendering improved pharmacokinetic properties to the modified drug delivery vehicle [139]. Additionally, leukocyte membrane proteins usually allow for the homing-into or targeting of tumor sites, with an increased circulation time. In fact, leukocyte membrane-modified nanoparticles have been reported to actively target tumor sites *in vivo* and therefore enable efficient drug delivery [140]. Cancer cell membrane-modified nanoparticles are also an attractive choice for the development of biomimetic nanoparticles; cancer cell membranes contain several cell adhesion molecules (integrins, cadherins, and selectins) [141], enabling the active targeting and selective uptake of nanoparticles in the tumor sites. Additionally, cancer cells also contain proteins that help evade immune recognition [142]. To coat cell membranes onto nanoparticle surfaces, the extrusion technique [143] (the cell membrane structures are repeatedly extruded with the nanoparticle of interest through porous membranes of varying diameter) or sonication [144] are usually employed to force an interaction between them.

Cell membrane vesicles as drug delivery vehicles. As an alternative to cell membrane coated nanoparticles, vesicular structures directly secreted by cells can also be used for drug delivery (Table 4). Since extracellular vesicles are released from cell membranes, they also harbor protein and lipid compositions, similar to those of the parent cell membrane. The main advantage is that these extracellular vesicles can be directly loaded with drugs or other functional nanoparticles and used for drug delivery applications. Among the different types of extracellular vesicles, exosomes are the most suitable for drug delivery applications because they are naturally utilized for non-contact intercellular communication and are of an optimum size range of 30–150 nm [149].

A previous study evaluated macrophage-derived paclitaxel-loaded exosomes for their therapeutic efficacy against multidrug-resistant cancer cells harboring drug efflux transporter

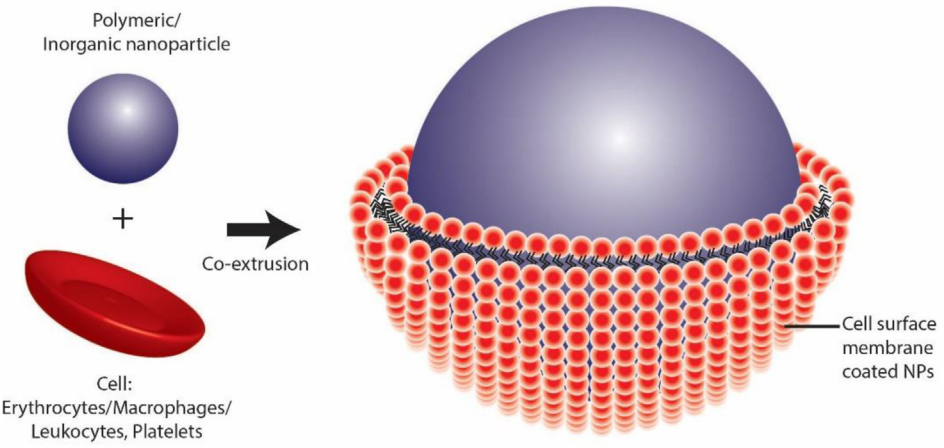

FIGURE 5

Cell membrane-coated nanoparticle.

TABLE 3

Cell membrane sources used for drug delivery/nanoparticle surface coatings.

Cell source	Loaded cargo/*loading method*	Cancer type	Remarks	Reference
Erythrocytes	Paclitaxel loaded polycaprolactone nanoparticles/*co-extrusion*	Breast (*in vivo* – 4 T1; dose: 10 mg/Kg)	Cancer metastasis treatment	[145]
Melanoma cancer cells	PLGA nanoparticle/*co-extrusion*	Melanoma (*in vitro* – dendritic and T-cell activation)	Anticancer immune activation	[146]
Mesenchymal stem cells	sTRAIL (soluble form of TNF-related apoptosis-inducing ligand)/*co-extrusion*	Prostate (*in vivo*- PC3; dose: 300 μg/mouse)	Single-dose administration elicits an effective response	[147]
Leucocytes	Nano-porous silicon/*overnight incubation at 4 °C*	Melanoma (*in vivo* – B16)		[148]
Platelets	Docetaxel or Vancomycin loaded PLGA nanoparticle/*bath sonication*	-	Treatment of coronary restenosis and bacterial infection	[144]

proteins [150]. Exosome loading was facilitated through sonication, with a high level of drug loading (~28%) when compared to other techniques such as incubation and electroporation. Of note, the accumulation/cytotoxicity of the drug-loaded exosomes was greater (*versus* the free drug), suggesting that the exosome packaging led to the entry of the drug into the cells through a different pathway. These drug-loaded exosomes were also found to significantly inhibit metastasis in a Lewis lung carcinoma mouse model. In another study, exosomes with tumor-targeting capabilities were isolated from dendritic cells expressing the iRGD peptide (to bind to alpha-V integrin-positive cancer cells) [151]. These exosomes loaded with doxorubicin when administered *in vivo* in a breast tumor mouse model accumulated preferentially at the tumor site, leading to a significant reduction in the tumor volume, when compared to that observed in the free drug and passively targeted exosome groups. Apart from the use of mammalian cell-derived exosomes, researchers have also highlighted the potential of exosomes derived from other biological sources, such as milk [152], plants [153], and fruits [154] for drug delivery.

A potential biomimetic material that has high translational capability owing to the ease with which large-scale synthesis and modifications can be done, are exosomes derived from bacterial sources, such as bacterial membrane vesicles. Recent reports have highlighted the capability of utilizing bacterial membrane vesicles for the delivery of siRNA for hepatocellular cancer [155], melanin for photothermal therapy of breast tumors [156], doxorubicin for lung cancer [157], and tegafur for breast cancer [158].

Non-polymeric nanoparticles/inorganic nanoparticles. Inorganic nanoparticles, including metal or metal-oxide nanoparticles (such as gold, iron oxide, and silica) and non-polymeric nanomaterials such as carbon nanotubes are also used for drug delivery. Apart from their large surface-area-to-volume ratio and many available functional groups, they possess unique optical and magnetic properties, which are considered an advantage in drug delivery applications (Table 5).

Gold nanoparticles. Gold nanoparticles have been widely explored for drug delivery applications owing to their high levels of biocompatibility, chemical stability, and easy synthesis. Using different reaction chemistries, gold nanoparticles of various shapes and sizes have been synthesized, including rods [179], triangles [180], stars [181], and core-shells [182]; their uptake by cancer cells and potential for cargo delivery have also been investigated [183]. Of note, the photothermal capability (generation of heat upon light exposure) of gold nanoparticles has been widely explored in the context of stimuli-responsive drug delivery (discussed below).

Iron-oxide nanoparticles. Like the gold nanoparticles, iron-oxide nanoparticles are easy to synthesize and biocompatible, making them suitable for drug delivery. Different formulations of such

TABLE 4

Cell membrane vesicles used for drug delivery applications in cancer therapy.

Cell membrane vesicle	Cell source	Loaded cargo	Cancer types	Remarks	Reference
Exosomes from mammalian cells	Dendritic cells	Doxorubicin	Breast (*in vivo*- MDA-MB-231; dose: 3 mg/Kg)		[151]
	Macrophages	Paclitaxel	Lung (*in vivo* – 3LL; dose: 50 mg/Kg)	Effective anti-metastatic response	[150]
	Prostate cancer cells	Paclitaxel	Prostate (*in vitro* - PC-3 and LNCaP)		[159]
	Reticulocytes	Doxorubicin	Liver (*in vivo* - H22; dose: 5 mg/Kg)	Magnetic field-assisted targeting and drug delivery	[160]
Bacterial membrane vesicles	*E. coli*	siRNA	Liver (*in vivo* – HCC-1954; dose: 4 μg/mouse)		[155]
	Klebsiella pneumoniae	Doxorubicin	Lung (*in vivo* – A549; dose: 2 mg/Kg)	Antitumor immune response	[157]
	Salmonella Typhimurium	Tegafur-loaded micelles	Melanoma and breast (*in vivo* – 4 T1, B16410; dose: 2 μg/mouse)	Antitumor immune response	[158]

nanoparticles have already been approved for clinical use, such as Ferumoxytol [184] for the treatment of anemia in patients with chronic kidney disease, Ferucarbotran [185] for liver MRI, Ferumoxsil [186] for gastrointestinal imaging, and NanoTherm [187] for hyperthermia therapy for recurrent glioblastoma multiforme. Their use in the clinics makes them attractive options for further studies of drug delivery applications. In addition to exhibiting magnetic contrast, these nanoparticles can also be engineered for stimuli-responsive magnetic hyperthermia [188] and magnetic tumor targeting [189] for drug delivery.

Mesoporous silica nanoparticles. Mesoporous silica nanoparticles are excellent vehicles for cargo delivery because they possess a high internal surface area and pore volume. Different reaction chemistries have been utilized to control the pore volume of these nanostructures, giving them a unique advantage over other conventional drug delivery vehicles [190,191]. In one such study [191], drug-loaded mesoporous silica nanoparticles of different pore sizes (~2, 5, and 8 nm) were synthesized and their therapeutic efficacy was evaluated for the treatment of hepatocellular carcinoma in mice. It was observed that higher drug loading could be achieved with both the 8 and 5 nm pore-sized nanoparticles when compared with the 2 nm pore-sized. However, efficient cellular uptake and eventual tumor therapeutic responses were significantly higher for the 5 nm pore silica nanoparticles. Such studies may support the development of effective drug delivery vehicles based on mesoporous silica nanostructures.

Nanocarbons. Nanocarbons, such as carbon nanotubes, carbon nanohorns (CNHs) graphene, and nanodiamonds (NDs), are widely studied in various research fields, including biomedicine, because of their unique physicochemical characteristics. Carbon nanotubes are one-dimensional nanostructures composed of graphene sheets that can either have single wall (diameter of 1–2 nm) or multi-wall structures (diameter of 10–100 nm). Owing to their one-dimensional structures, they behave differently from their spherical nanoparticle counterparts and they have the potential to exhibit efficient cell uptake due to their ultra-high surface area and chemical functional groups [192]. Single-walled carbon nanotubes specifically show unique optical properties that allow for their use in various applications such as photothermal therapy [193], photoluminescence [194], and photoacoustic imaging [195]; therefore, they are suitable for stimuli-responsive drug delivery. In fact, carbon nanotubes have been explored for the delivery of various types of cargo to cells, including therapeutic nucleic acids [196], proteins [197], and chemotherapeutic drugs such as paclitaxel [198] and doxorubicin [199].

Meanwhile, CNHs are aggregates of graphitic tubes with closed ends and cone-shaped caps (horns). Each tube has a diameter of 2–5 nm, and the aggregated tubes form spherical structures (about 80–100 nm in diameter). This aggregate size is suitable for eliciting the EPR effect. Moreover, the external surface and/or inner spaces of CNHs can be easily loaded with anticancer drugs for slow release [200–202]. Importantly, CNHs do not exhibit toxicity, making them appropriate for drug delivery systems. Miyako and his team [175] found that functional CNHs exhibit attractive photothermal conversion properties and paramagnetism; they allowed the release of drugs and the manipulation of enzymatic reactions at the target site in transgenic mice using biologically permeable NIR light and magnetic fields. Interestingly, the authors synthesized a supramolecular nanoconjugation of temperature-responsive liposomes and magnetic nanoparticle- and polyethyleneimine (PEI)-decorated CNHs through avidin and biotin interactions (Fig. 6).

The photothermal conversion of CNH itself not only effectively allows the hyperthermic elimination of cancer cells [203–205] but it also allows for target gene transduction through the inoculation of genetically engineered cells with a heat-shock promoters [206]. Furthermore, Miyako and his team [207] recently discovered that the NIR light-induced and antibody-functionalized CNH nanocomplexes photothermally trigger calcium influxes into target cancer cells overexpressing the transient receptor potential vanilloid family type 2 (TRPV2) (Fig. 7). This combination of the optical property of CNH and genetic engineering effectively eliminates cancer cells and inhibits their stemness *in vitro* and *in vivo*.

Graphene and graphene oxide are also promising drug delivery carriers because they exhibit good biocompatibility and biodegradability as well as large surface areas, which allows for an increased loading of anticancer drugs through π-π stacking, hydrophobic interactions, and/or covalent conjugations with

TABLE 5

Inorganic/non-polymeric nanoparticles for drug delivery.

Inorganic nanoparticle	Reaction chemistry/nanoparticle type	Surface ligand	Stimuli-based drug delivery	Reference
Gold	Turkevich chemistry	4-(2-(6,8-Dimercaptooctanamido)ethylamino)-3-methyl-4-oxobut-2-enoic acid bound to doxorubicin	pH and NIR	[161]
	Turkevich chemistry	Peptide substrate, CPLGLAGG bound to doxorubicin	MMP-2 and GSH	[162]
	Star shaped gold NPs	Glutathione stabilizer bound to RGD peptide and doxorubicin	NIR Laser	[163]
	Rod shaped gold NPs	Carboxyl surface bound to CXCR4 antibody	NIR Laser	[164]
Mesoporous silica	Tetraethyl orthosilicate (TEOS) as the precursor	3-Aminopropyltriethoxysilane stabilizer bound to gold nanoparticles	Low pH and high ATP	[165]
	TEOS as the precursor	Thermosensitive linker 4,4′-azobis(4-cyanovaleric acid)	Ultrasound	[166]
	TEOS as the precursor	Carboxyl functional NP surface bound to Gd^{3+} ions and chlorin e6	NIR light	[167]
	Hollow mesoporous organosilica NPs (HMONs)	Protoporphyrin and RGD-targeting ligand	Ultrasound	[168]
Iron oxide	Co-precipitation technique	Carboxymethyldextran conjugated to EGF protein	Magnetic field	[169]
	MagForce® MFL AS	Aminosilane-coated NPs	Magnetic field	[170]
	Co-precipitation technique	Camptothecin drug linked to amino-poly(vinyl alcohol)	Magnetic field targeting	[171]
Nanocarbon	Single-walled carbon nanotubes (SWCNT)	Surface modified to incorporate siRNA and NGR-targeting peptide	NIR laser	[172]
	Multi-walled carbon nanotubes (MWCNT)	PAMAM dendrimers coupled to folic acid	Low pH	[173]
	Graphene	Doxorubicin covalently bound to the graphene surface	NIR laser	[174]
	Carbon nanohorn (CNH)	Magnetic nanoparticle-modified CNH conjugated with temperature-responsive liposome encapsulating drugs	NIR laser and magnetic field	[175]
	Nanodiamond (ND)	Photosensitizer and paclitaxel functionalized ND	NIR laser	[176]
Ga-based LM NPs	Eutectic gallium-indium (EGaIn)	$DSPE\text{-}PEG_{2000}$-amine; DC(8,9)PC	NIR laser	[177]
		MUA-CD;m-HA	Low pH	[178]

NP, nanoparticle; NGR, Asn-Gly-Arg; LM, liquid metal.

functional molecules. Indeed, the targeted delivery of drug-loaded graphene and graphene oxide has previously been explored as a cancer chemotherapy [208–211]. For example, an interesting strategy to enhance the targeting and pharmaceutical efficacy of graphene is the use of multi-chemical functionalization with indocyanine green (ICG), folic acid, and doxorubicin [174]. The multi-functional graphene nanoconjugates exhibit remarkable targeting capacities alongside a synergistic effect of the drug release and photothermal conversion, highlighting the advantage of combining chemo- and phototherapies against cancer.

Finally, NDs, with individual diameters of 2–10 nm and a truncated octahedral structure, have significantly contributed to the development of highly efficient and successful drug delivery systems owing to their relatively low costs, amenability to large-scale synthesis, unique structures, and low toxicity. Indeed, anticancer drug formulations with NDs are promising because of their uniform and tunable sizes, high drug loading capacities, and efficacy as a drug delivery system [212–216]. Functionalized NDs spontaneously transform into well-dispersed and biocompatible supraparticle nanoclusters via simple chemical conjugations with perfluorooctanoic acid [217], amphipathic molecules [218,219], or organic dyes [176]. Notably, drug-loaded ND supraparticles can improve anticancer drug efficacy because of their higher capacity for intracellular invasion when compared with that of pristine NDs without any chemical functionalization. Of note, encapsulating molecules into the nano spaces of these conventional nanocarbons requires complicated processes, such as the preparation of open holes, vacuum heating, and nanoprecipitation methods. In contrast, drug-conjugated ND supraparticles can be easily synthesized by simple sonication. Thus, the concept and design of ND supraparticles should be considered for the generation of practical drug delivery systems to treat a range of cancers.

Liquid metal (LM) nanoparticles. LMs are emerging materials that have attracted considerable attention. LMs and their metal alloys have low melting points and are thus in the liquid state at near-room temperature. Gallium and mercury and their alloys are representative LMs. Among which, Ga-based LM nanoparticles (LMPs), especially eutectic gallium-indium (EGaIn) and gallium-indium-tin (Galinstan) nanoparticles have been widely applied in different therapeutic areas, including drug delivery, tumor ablation, X-ray CT imaging, photoacoustic imaging, MRI, and biosensing due to their plasmonic effect and electromagnetic and electrochemical properties. For example, Lu et al. [178] utilized two types of thiol ligand-thiolated (2-hydroxypropyl)-b-cyclodextrin (designated MUA-CD) and thiolated hyaluronic acid (designated m-HA) to load anticancer drugs for targeted delivery to solid tumors in mice. The acidity of the tumors leads to the controllable release of drug molecules from Ga-based LMPs.

Other strategies for exploiting the potential Ga-based LMPs include the application of physical stimuli such as light [177,220–222], electromagnetic fields [223–225], and acoustic waves [177,221,226,227] for drug delivery, cancer treatment, bioimaging, or biosensing. For instance, Chechetka et al. [177] demonstrated that photo-polymerized EGaIn nanoparticles encapsulating anticancer drugs can generate heat and reactive

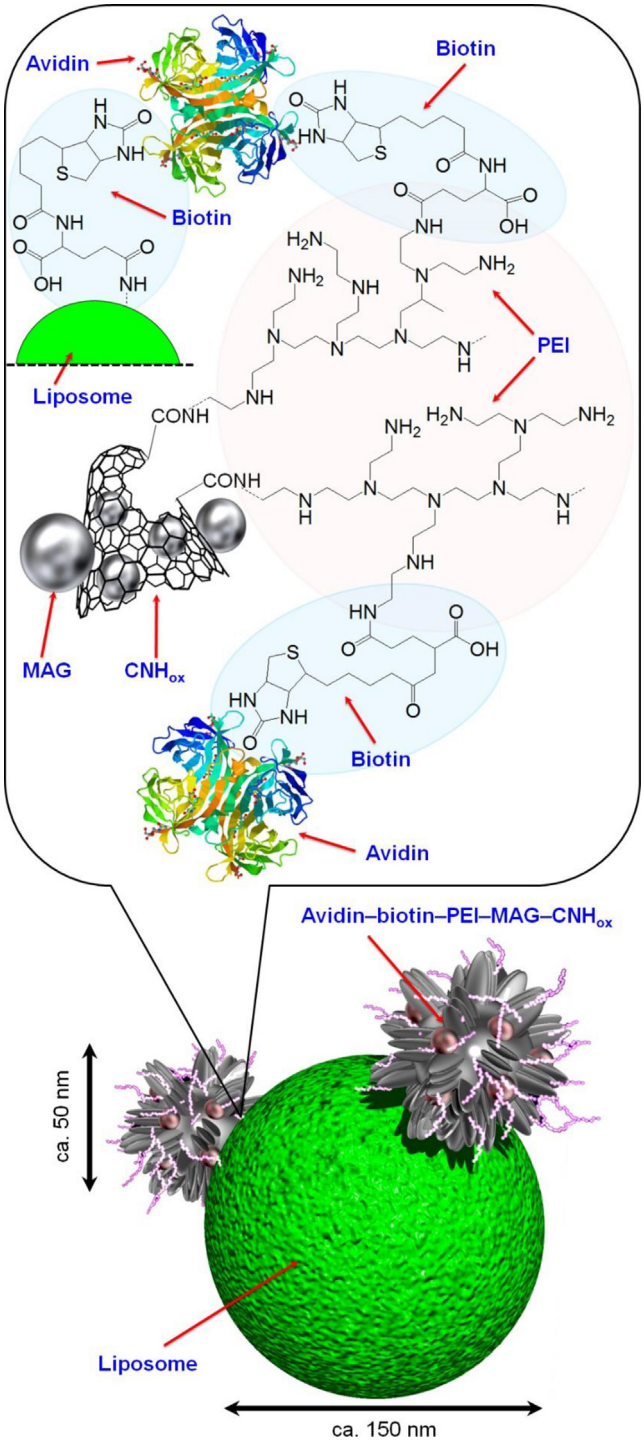

FIGURE 6

Schematic illustration of the CNH and liposome nanocomplex. Reproduced with permission from Chechetka et al. [175], copyright (2016), Wiley.

oxygen species (ROS) under biologically permeable NIR laser irradiation. To express the multiple functions of LM, 1,2-distearoyl-sn-glycero-3-phosphoethanolamine-N-[amino(polyethylene glycol)2000] (DSPE-PEG_{2000}-amine) and 1,2-bis(10,12-tricosadiynoyl)sn-glycero-3-phosphocholine (DC(8,9)PC) were used to prepare EGaIn/polymer core–shell nanostructures via 254 nm ultraviolet curing (Fig. 8). Of note, the shape of photo-polymerized EGaIn nanoparticles can be drastically changed via NIR laser irradiation; the nanostructures are destroyed for the controlled spatiotemporal release of the loaded drugs at the target site. EGaIn nanoparticles also have several unique functions, in addition to their photothermal and chemotherapeutic effects for cancer elimination; for instance, they were used as X-ray and photoacoustic contrast agents in biological organs and mice. Furthermore, Chechetka et al. [177] successfully controlled intercellular calcium ion fluxes using LMs. Meanwhile, Yu et al. [223] found that the electromagnetic field can induce powerful eddy-thermal effects in the context of EGaIn composites for biomedical applications. In fact, this exothermic phenomenon makes them promising candidates for controlled drug release and hyperthermic cancer therapy. These studies offer prospects for the use of Ga-based LMPs as advanced drug delivery systems.

Nanoscale Metal-Organic Frameworks. Nanoscale Metal-Organic Frameworks (nMOFs) are materials that are formed due to the self-assembly of a multitopic organic linkers with multi-valent metal ions (nodes) leading to the generation of a highly porous three-dimensional structural framework. nMOFs have widespread applications, predominantly in the fields of catalysis, energy storage and gas separation, and more recently drug delivery. This is primarily because they have large internal surface areas unlike other nanoparticle structures [228], which can enable high levels of drug loading and delivery. Drug encapsulation in nMOFs has been demonstrated using several routes (Fig. 9). In one example, the encapsulation of the anti-cancer drug campothecin within the pores of spherical zeolitic imidazole framework-8 (formed by 2-methyl imidazolate and zinc ions) nanostructures was reported by the simple introduction of the drug during nMOF synthesis [229]. These highly monodispersed 70 nm drug loaded nMOFs showed a significantly higher cell death response for MCF-7 breast cancer cells when compared to unloaded nMOFs. Additionally, the co-loading of magnetic iron-oxide nanoparticles with fluorochrome molecules within these nMOFs were also demonstrated which showed dual magnetic targeting and imaging capabilities, thus highlighting the highly porous nature of these structures. However, the encapsulation of drug/cargo in nMOFs during their synthesis requires that the cargo of interest does not degrade during the process which generally involves a solvothermal technique. To counter this, post-synthesis modifications of nMOFs can be employed wherein these materials act as 'molecular sponges' [230]. In this extensive report by Horcajada et. al., different nMOFs based on Fe (III) precursors and various organic linkers were synthesized and loaded with anti-cancer drugs by incubating the dried nMOFs in drug solutions at room temperature. Specifically, high drug loading capacities for busulfan (31.9%) and doxorubicin (11.2%) could be achieved in the nMOFs synthesized with tritopic trimesic acid as the organic linker. In this case, the drug release from the nMOFs was found to be mainly because of the diffusion of the drug from its pores and not because of its degradation. In cases where the pore sizes of the synthesized nMOFs were smaller than the drug that was to be loaded, surface modification strategies could be employed. Here, the presence of coordinately unsaturated metal centers at the outer surface of the nMOFs could be advantageously utilized to directly load drugs or other linker molecules (e.g., polymers, amino acids etc.) onto the surfaces of the nMOFs. In one such study, the post-synthesis

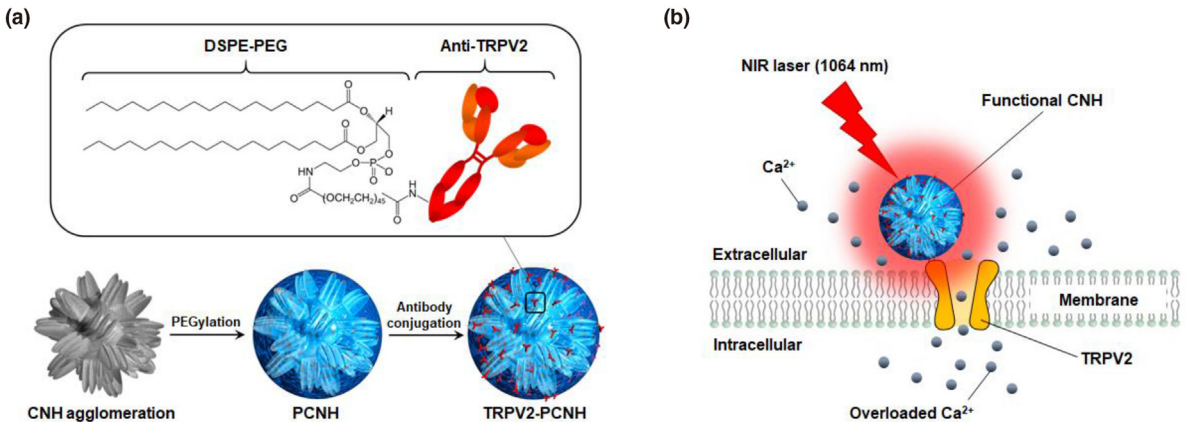

FIGURE 7

CNHs for cancer therapy. (a) Schematic illustration of the CNH nano-conjugation structure. (b) Mechanism of cancer cell death that is triggered by the photothermal properties of CNH and temperature-sensitive TRPV2-mediated Ca^{2+} overdosing. Reproduced with permission from Yu et al. [207], under the creative commons attribution license.

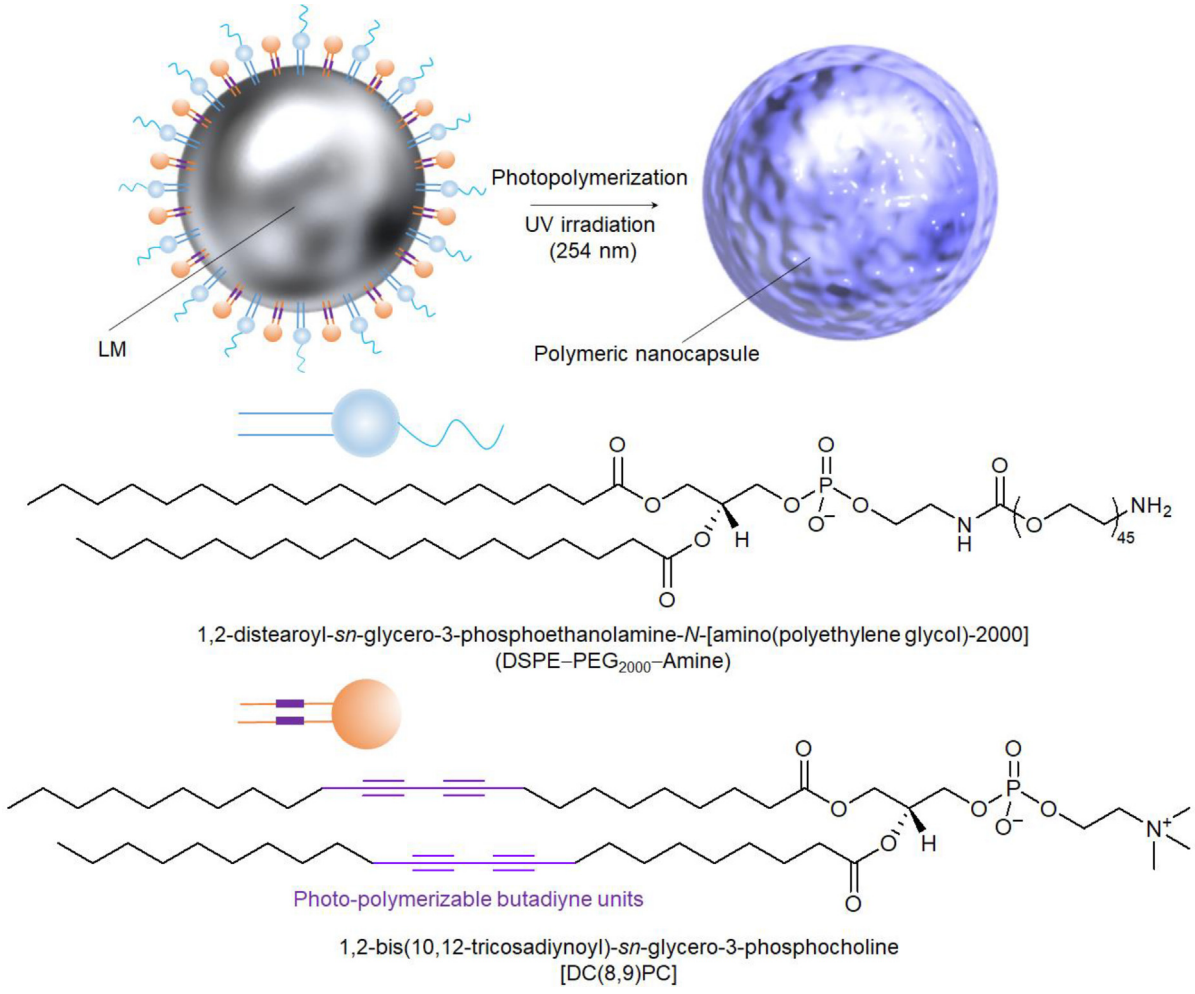

FIGURE 8

Liquid metal (LM) nanocapsule components including EGaIn, DSPE-PEG2000-amine, and DC(8,9)PC. The polymeric core–shell structure encapsulating the LM is prepared by crosslinking the butadiyne moieties from DC(8,9)PC using 254 nm ultraviolet irradiation. Reproduced with permission from Chechetka et al. [177], under the creative commons attribution license 4.0.

loading of a dried zeolitic imidazolate framework (ZIF-8; that consists of Zn^{2+} as the metal nodes) with doxorubicin, showed that drug loading was predominantly achieved at the surface of the nMOFs, and this was further confirmed through molecular

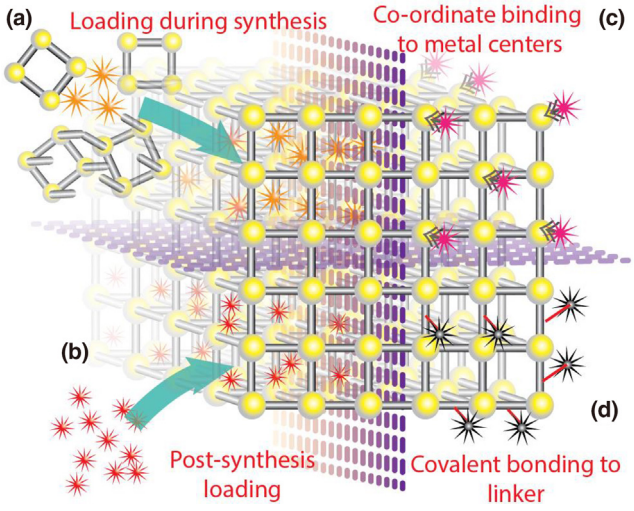

FIGURE 9

Different strategies by which nMOFs can be loaded to include drugs. (a) Drug loading during nMOFs synthesis, (b) drug loading after the synthesis of nMOFs, (c) Co-ordinated binding of the cargo to metal centers in the nMOFs, and (d) covalently binding cargo to the nMOF linkers.

docking studies [231]. In a similar study, MIL-101 nMOF containing Fe^{3+} metal nodes were coupled with selenium and ruthenium nanoparticles which showed anticancer activity. This was achieved by first coordinatively binding and grafting of cysteine to the nMOFs followed by a reduction in selenium and ruthenium salts on the grafted surface [232]. Alternatively, the binding of drugs onto the nMOF surfaces can also be accomplished through covalent conjugation by utilizing functional organic linkers as building blocks. This was demonstrated in a study wherein MIL-101 structures were synthesized introducing 2-amino terephthalic acids additionally as linkers instead of the terephthalic acid alone, as they provided crucial amine functional groups for further modification [233]. Carboxyl functionalized cisplatin was then covalently conjugated to nMOF at a high drug loading capacity of 12.8%. This and other techniques have been reported widely in the literature to demonstrate the utility of nMOFs for anti-cancer drug delivery [234,235].

Stimuli-responsive drug delivery. As mentioned previously, the overall goal of any nano-drug delivery system is to improve the pharmacokinetic properties of the loaded drug by enhancing its concentration at the tumor site while minimizing off-target toxic effects. The successful delivery of drug-loaded nanoparticles at the tumor site, however, is mostly dependent on the tumor biological characteristics such as the EPR and tumor perfusion. By using targeted nanoparticles that are surface-modified with ligands to bind to the tumor cell receptors, effective and increased cell internalization of the nanoparticles could be achieved. However, even then, the ability of the nanoparticles to reach the tumor site is still predominantly dependent on their passive targeting ability [236]. One way of maximizing the accumulation of drugs at the tumor site is to promote maximum drug release at the desired site. This can be achieved by using stimuli-responsive nano-drug delivery vehicles that can promote on-demand drug release at the tumor site in the presence of a stimulus. Such nanoparticles enable spatiotemporal control over drug release and are considered as the next-generation drug delivery system, with the potential to significantly improve therapeutic responses. Different types of stimuli-responsive nanoparticle systems have been investigated based on the stimuli used to trigger drug release: internally (based on the tumor characteristics) or externally (delivered from outside the body) (Fig. 10).

The tumor microenvironment possesses specific characteristics, different from those of the surrounding environment. These differences occur due to the high growth rate and metabolism of tumor *versus* normal cells. The high metabolic state leads to the generation of high concentrations of lactic acid, resulting in an acidic (low pH) state within the tumor microenvironment (Warburg effect [237]). Therefore, pH-responsive drug delivery systems that undergo disintegration in low pH conditions leading to drug release would be useful. Furthermore, this has been widely demonstrated in the context of pH-sensitive polymers as building blocks or with acid-labile chemical bonds that are used to conjugate the drug to the delivery system [238]. Another distinctive characteristic of many tumor types is the elevated levels of glutathione and the consequently high reducing environment within the tumor mass [239]. In line with this fact, to enable controlled drug delivery, reports have highlighted the incorporation of glutathione-cleavable dithiol functional groups [240] within the delivery vehicle, aiming at its disintegration and eventual drug release. In one such report, dithiol functional groups were incorporated to form cross-linked polymeric micelles which not only showed an enhanced circulation time of the loaded doxorubicin drug, but importantly lead to a significant reduction in M109 tumor volumes when used in-vivo and compared to self-assembled micelles without a dithiol functional group [241]. Another intrinsic tumor characteristic is the presence of elevated levels of enzymes such as matrix metalloproteinases (MMP-2, MMP-9) [242] and cathepsin-B [243]; and the incorporation of such specific enzyme-cleavable functional groups within the delivery system can be used to achieve stimuli-responsive drug delivery [244].

Although the use of stimuli-responsive nanoparticles based on intrinsic stimuli is an attractive option, intra- and inter-tumoral differences (e.g., pH and enzyme levels) can markedly affect their therapeutic efficacy, thus posing a major barrier to clinical translation [236]. Considering this, the remote use of external stimuli to control drug release is a more feasible option. Of note, such externally controllable stimuli can be modulated allowing spatiotemporal control to maximize the desired therapeutic outcome. These stimuli (investigated for controlled drug release) include NIR light, magnetic fields, and ultrasonic waves (Fig. 10); theoretically, they must exhibit good tissue penetrability without causing any adverse effects. NIR light (800–1000 nm wavelength) has been widely investigated in conjunction with the use of anisotropic gold nanoparticles (nanorods [245], core/shells [246], nanostars [247]), with a corresponding absorbance in the NIR window due to a longitudinal surface plasmon resonance effect. The absorption of NIR light by gold nanoparticles can, thus, lead to the generation of a highly localized temperature elevation [248] and hyperthermia-induced cell death. Additionally, when using gold nanoparticles as drug carriers, alone or in combination with drug delivery depots (e.g., polymeric drug

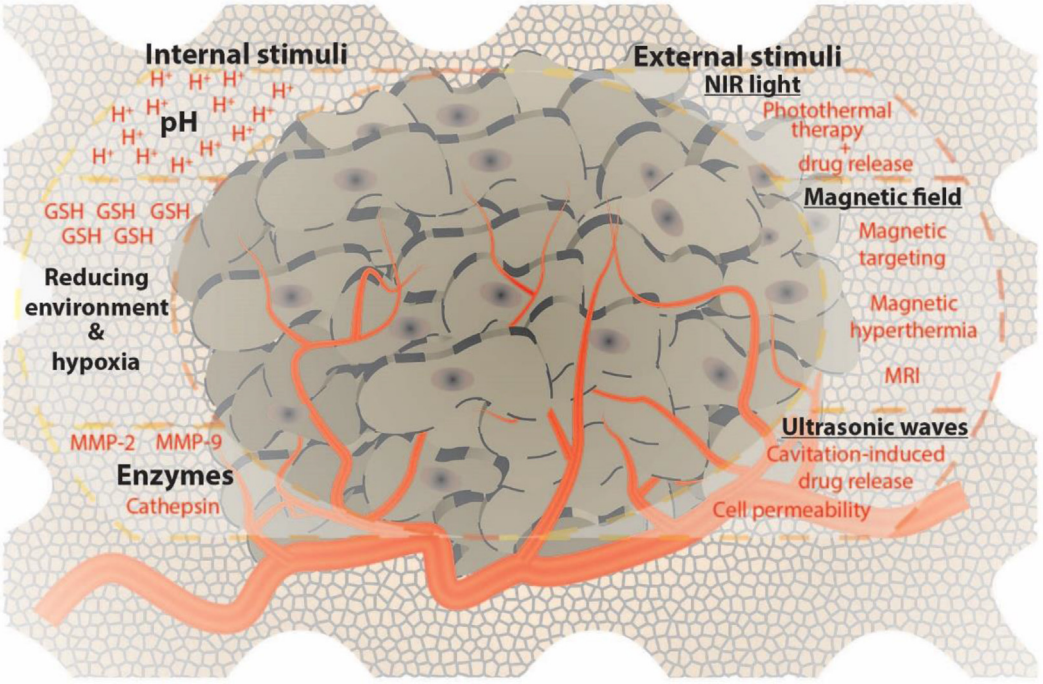

FIGURE 10

Different types of internal and external stimuli that can be used to design smart drug delivery systems for on-demand drug release.

delivery systems [249]), NIR light-induced stimuli-responsive drug release can be achieved, which can lead to increased therapeutic efficacy due to the synergistic effects of hyperthermia and drug toxicity [250]. The use of magnetic fields as an external stimulus provides a more versatile option for drug release in the context of magnetic nanoparticles. By applying alternating magnetic fields, hyperthermia effects can be induced using magnetic iron-oxide nanoparticles [251], and when utilized as a drug carrier, they can aid in remote-controlled drug delivery. Additionally, via the exposure of the tumor mass to magnetic fields, magnetic targeting [252] and improved localization of the magnetic iron-oxide nanoparticle is possible, which promotes drug accumulation at the tumor site. These magnetic iron-oxide nanoparticles can also be used as contrast agents for magnetic resonance imaging and can, therefore, be used for combined therapy and diagnostic applications (theranostics [253,254]). Finally, the use of ultrasound as an external stimulus for triggering drug release has also been explored as a viable, clinically translatable option. Ultrasounds destroy the accumulated drug carrier at the diseased site, leading to (burst) drug release [255]. Importantly, the effectiveness of such stimuli has been demonstrated in the context of liposomes [256] and micelles [257] as drug carrier vehicles. Of note, via the modulation of the ultrasound frequency and intensity used, the resulting cavitation-mediated microbubbles can lead to the formation of reversible pores on cell membranes, improving drug/nanoparticle internalization at the tumor site [258].

Summary of different nanomaterial systems. Among the different nanomaterials used for drug delivery applications that have been discussed here, each has multiple advantages and disadvantages (Fig. 11). The use of a specific type of material for a cancer therapy ultimately depends upon the net intended application which could include drug delivery, active targeting, imaging, immunotherapy, and controlled long-term drug release. In the present research landscape, it is important to note that almost all nanomaterials investigated for drug delivery are engineered to possess multi-functionality, either though the addition of multiple functional chemical/biological groups (e.g., pH responsive polymers, enzyme cleavable linkers, antibody ligands, etc.) or through the combination of different nanomaterials to form a hybrid/composite nanostructure. Two primary reasons could be considered for this shift in outlook: (a) the benefits of adding multiple functionalities (e.g., combined therapy and imaging, remote-controlled stimuli-responsive drug delivery) seem to show a multi-fold increase in therapeutic outcomes when compared to single-functional nanosystems; and (b) the improvement and increase in knowledge relating to the synthesis chemistries when combining multiple materials in one single platform. Even though these advantages have been highlighted in multiple studies for multi-functional/stimuli-responsive nanomaterials, a corresponding increase in the clinical translation of such systems is suffering from multiple bottlenecks. One of the biggest disadvantages of utilizing multiple components to synthesize a specialized nanomedical system is the difficulty in determining the safety profile of every component encompassing the system. The other major disadvantage is the complexity related to the scale up of the synthetic chemistries of such systems that tend to become more difficult with the addition of multiple components. Nevertheless, it is important to realize that these nanomedical systems show great promise in treating cancers which are difficult to treat using conventional treatment

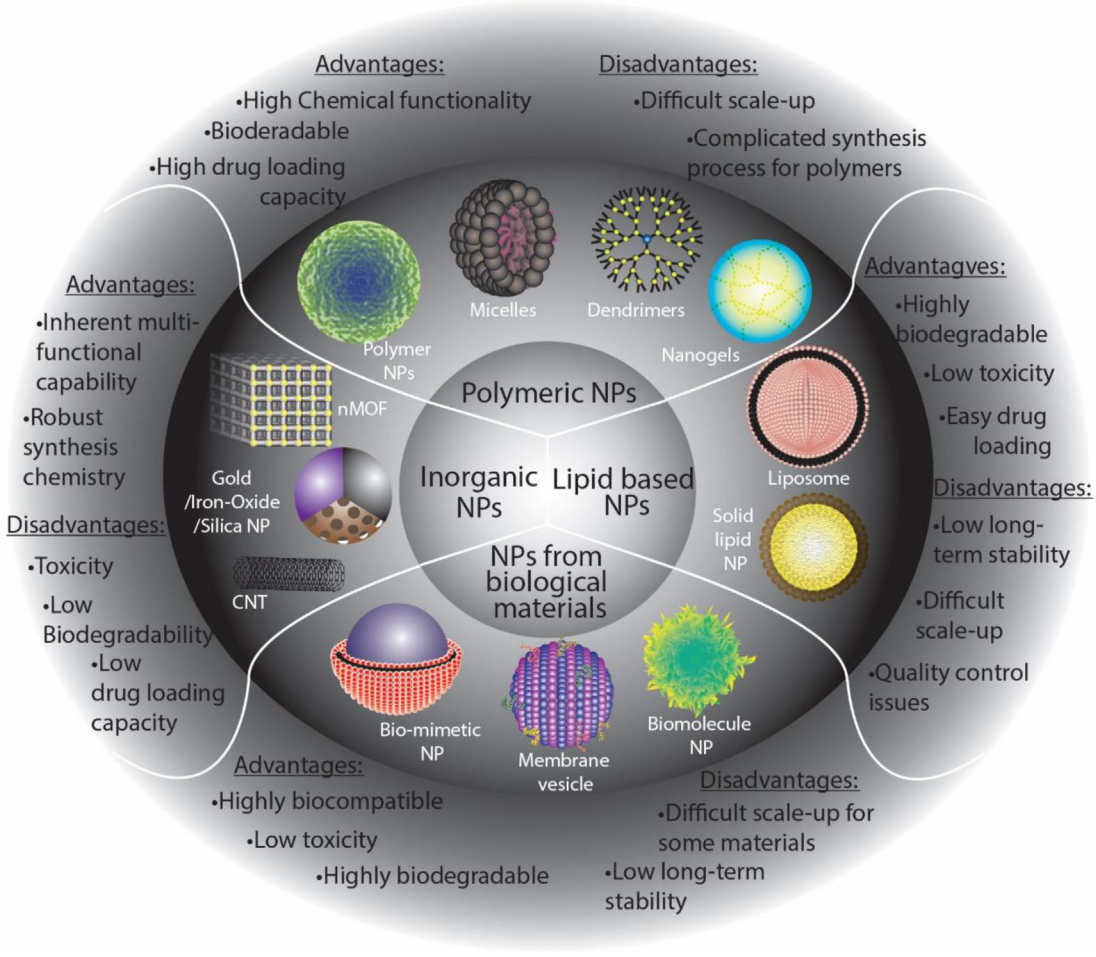

FIGURE 11

Summary of the advantages and disadvantages of the different nanomaterial systems used for cancer therapy.

modalities but the transition from the bench to the bed-side requires more research and a clearer understanding of their cost-to-benefit ratios.

Material-based cancer immunotherapy

Cancer immunotherapy relies on the ability of the body's immune system to fight against cancer accurately and safely. In the previous two decades enormous progress has been made in relation to cancer immunotherapy and this has resulted in advances and positive outcomes [259–261]. Drugs are designed to incite healthy primary and secondary antitumor immune responses via the revamping/improvement of natural mechanisms that are altered in cancer foci, thus constraining tumor growth and metastasis [262]. Therefore, the development of cancer immunotherapy approaches depends on our understanding of the relationship between the immune system and cancer, famously known as the cancer-immunity cycle [263]. The first cancer immunotherapeutic drug, the cytokine interferon-α (IFN-α) was approved by the FDA for the treatment of hairy cell leukemia [264]. However, there are several problems associated with immunotherapeutic drugs, such as the large dose requirement due to their short half-life which causes autoimmune side effects, their limited effectiveness (in few patients), and the restricted use of the treatments for hematological tumors, due to the complex tumor microenvironment (TME) of solid tumors [265].

To overcome such side effects and improve the efficacy/accuracy of immunotherapy approaches, novel drug delivery systems (DDS) are required. In recent years, DDSs were designed for the prolonged release of immunotherapeutic drugs *in vivo* [266]; a variety of biomaterials-based systems have been developed including liposomes, hydrogels, polymers, and silica nanorods (Table 6) that have improved capacities for the specific and targeted delivery of drugs, low toxicity, high efficacy, and immune-stimulating effects [266,267].

Recently, it was found that combined photothermal immunotherapy could enhance the antitumor immune response and overcome the problems associated with photothermal therapy (PTT) [285–290]. Li et al. prepared nanofibrils by assembling immunomodulatory thymopentin (TP5) and ICG (TP5-ICG NFs) for combined NIR photothermal immunotherapy to treat pancreatic cancer. The TP5-ICG NFs showed promising results by inhibiting the tumor growth, removing tumor metastasis, and minimizing the side effects after single injections and one irradiation (Fig. 12) [291]. Li et al. also showed that fluorophore-loaded liposomes (IR-7-lipo) tailored with an immunoadjuvant (HA-

CpG) could increase the efficiency of $CD8^+$ T effector cells and alleviate the immunosuppressive TME [292]. Luo et al. developed an anti-PD-1 peptide (AUNP12) in the context of a hollow gold nanoshell co-encapsulated with PLGA NPs; these nanoparticles potentiated the inhibition of primary and distal tumor growth by increasing the percentage of $CD8^+$ CTLs and the secretion of IFN-γ [293]. Furthermore, iron oxide NPs can be used concurrently for cancer immunotherapy and imaging; in fact, these NPs have been approved as MRI contrast agents and their degradation products are beneficial for the body's iron storage [294].

Although cancer immunotherapy is attracting increasing amounts of attention, there remains a huge gap between human patient treatments *in vivo* and *in vitro* laboratory models, as very few formulations are undergoing clinical trials. Indeed, resources for the development of biomaterials for DDSs are available; however, the economical large-scale production of such materials is still challenging. Therefore, there is an urgent need for new cost-effective materials and humanized models for the appropriate development of efficient and potent immunotherapy-based cancer treatment options.

Materials as direct therapeutic agents

Anticancer cationic peptides

Peptides consist of short chains of 5–50 amino acids linked via peptide bonds and they are mainly arranged in one of two secondary structures, α-helices or β-sheets. In addition, peptides possess distinctive features, such as hydrophobicity and high cationic charges, which facilitate the formation of amphiphilic structures and interactions with cancer cells [295,296]. Materials based on peptides were, not surprisingly, found to be promising as anticancer agents, due to their easy delivery, optimal sensing, fate control, and tumor tissue perforation, and the generation of immunological responses [297–300]. Tumor cells differ from normal cells in their morphological appearance, have different chemical compositions and cellular membranes, and lose their original functions. Anionic molecules such as phospholipid phosphatidylserine, O-glycosylated mucins, heparin sulfate, and sialylated gangliosides are overexpressed in cancer cell membranes, resulting in a net negative charge when compared to normal cells. Due to these key differences between normal and cancer cells, it has been predicted that cancer cells are more vulnerable to anticancer cationic peptides (ACPs), resulting in the likelihood of selectivity. In the following sections, the different modes of action for the anticancer peptides are discussed.

Membranolytic mechanism. Peptides with membrane-disrupting lytic modes of action serve as defense molecules in plants, invertebrates, vertebrates, bacteria, insects, and humans. These membrane lytic peptides have gained recognition as antimicrobial peptides and can affect both eukaryotic and prokaryotic cells. Subsequently, the sensitivity of tumor cells to ACPs was discovered. As discussed above, the negatively charged membranes of cancer cells bind to ACPs through electrostatic interactions, ultimately leading to cell membrane lysis. ACPs can interact with cancer cells through different mechanisms (Fig. 13) [301], such as the barrel-stave model, carpet-like mechanism, toroidal pore model, in-plane diffusion model, and detergent-like effect model (Table 7) [302].

TABLE 6

Different biomaterials used as drug delivery carriers for cancer immunotherapy.

	Type	Agents Delivered	Key Findings	References
Lipid-based biomaterials	Liposomes	CpG-ODN, IFN-γ genes, TGF-β inhibitor, IL-2, HA-CpG	Inhibition of tumor growth via increases in tumor antigen-specific $CD8^+$ cytotoxic T cells	[268,269]
	Lipid/calcium/phosphate (LCP) nanoparticles	Anti-CTLA-4 monoclonal antibody, Trp2, CpG-ODN	Modulation of TME	[270,271]
Polymer-based biomaterials	Micelles	Trp2, IFN-γ, CpG, OVA, STAT3 siRNA	Reduced immunosuppression in the TME Stimulation of CTL responses	[272,273]
	Nanoparticles	CpG ODNs, DPPA-1, NLG919, IFN-γ, OVA, anti-PD-1 monoclonal antibody	Promotes the maturation of DCs Enhances immunostimulatory effects of CpG under near-infrared (NIR) laser irradiation Inhibits tumor growth by increasing tumor antigen-specific $CD8^+$ cytotoxic T cells	[274-276]
	Hydrogels	IFN-α, GM-CSF, CpG-ODN, TCL, TLR3 agonist,	Survival and activation of CTLs Inhibits tumor proliferation via the coadministration of sorafenib Recruitment and activation of DCs	[277,278]
Inorganic biomaterials	Siliceous nanoparticles	GM-CSF, CpG, TRP2, TLR agonist, tumor vaccine	Increased efficiency of TRP2-specific $CD8^+$ T cells Stimulates better antigen-specific CTL responses, and delays tumor growth	[279,280]
	Iron oxide nanoparticles	CpG-ODN, ICG	Promotes immune cell activation Increases the efficiency of TRP2-specific $CD8^+$ T cells Integration of imaging and therapy	[281,282]
Microneedles	Hyaluronic acid (HA)-based	anti-PD-1 monoclonal antibody	Triggers inhibitory signaling downstream of the T-cell receptor (TCR) Prevents the activation of T-lymphocytes.	[283,284]

CpG ODN, Unmethylated cytosine-phosphate guanine oligodeoxynucleotide; TGF-β, Transforming growth factor-b; TCL, Tumor cell lysate; TRP2, Tyrosinase-related protein-2; TLR, Toll-like receptor; OVA, Ovalbumin; IL-2, interleukin-2; CTLA-4, Cytotoxic T-lymphocyte-associated protein-4; CTL, cytotoxic T-lymphocyte.

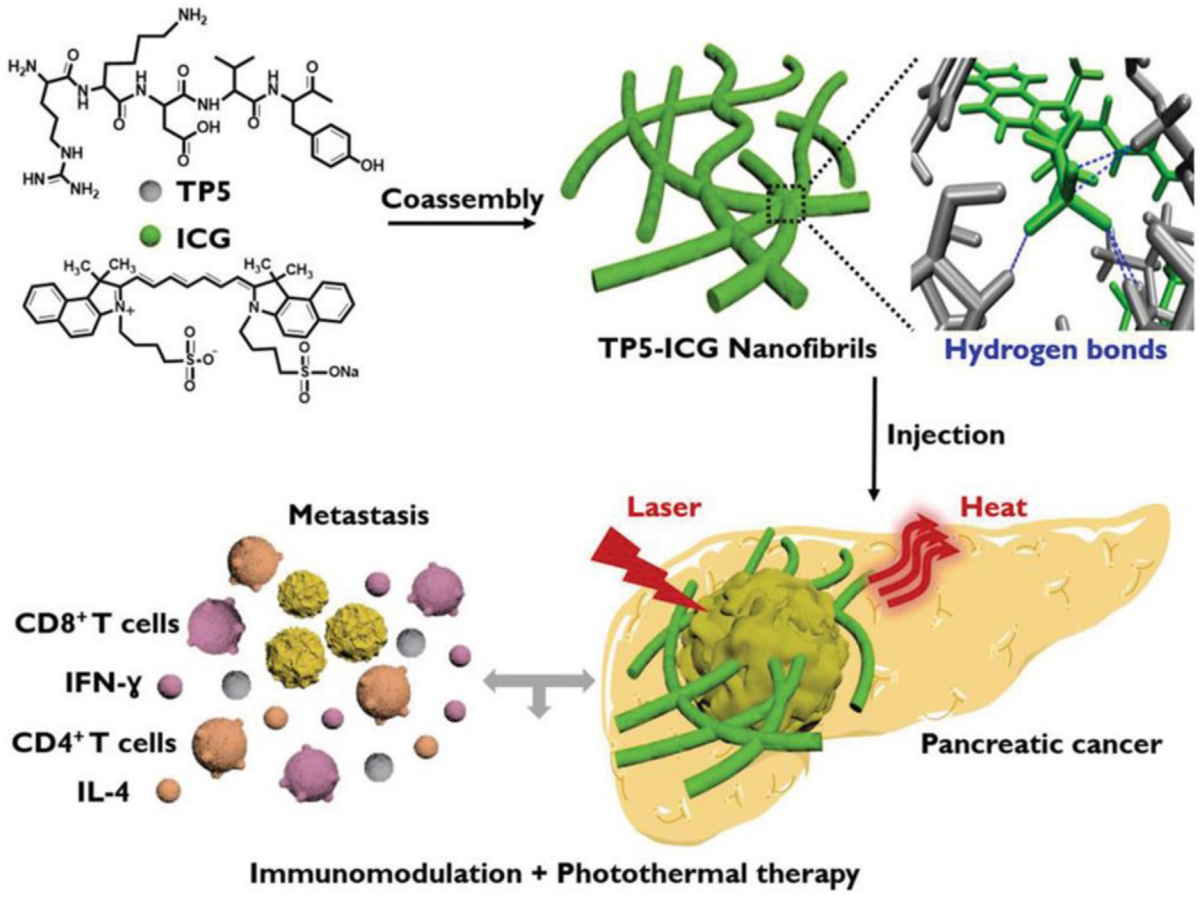

FIGURE 12

Mechanistic illustration of the formation and application of thymopentin-based near-infrared photothermal immunomodulatory nanofibrils. Reproduced with permission from Li et al. [291], copyright (2016), Wiley.

One of the initial findings in this field was reported by Cruciani et al. [314], who demonstrated the activity of ACPs against both hematopoietic and solid tumor cells. The authors performed cytotoxicity assays on several solid and hematopoietic tumor cell lines using nine magainin peptide analogs; cytotoxicity was observed within minutes against various cell lines. This activity of the magainin peptide has been shown in several studies by other research groups [314–317].

In another report, van Zoggel et al. [318] discovered the antiproliferative activity of dermaseptins, obtained from skin secretions of a frog (*Phyllomedusa bicolor*) from South America. Dermaseptins B2 (Drs B2) and B3 (Drs B3) of the dermaseptin B family were the focus of this research. The initial sequence analysis revealed two antimicrobial α-helical cationic peptides (dermaseptins B2 and B3). *In vitro*, the proliferation of the human prostatic adenocarcinoma PC-3 cells was controlled by these two synthetic B2 and B3 dermaseptins by more than 90% with an EC_{50} of approximately 2–3 μM. Of note, when tested in the context of NIH3T3 non-cancerous mouse cells, B2 had no effect, whereas B3 had a slight inhibitory effect at high doses. In another study, van Zoggel et al. [319] also found that Drs B2 hinders the proliferation and colony formation of several cancer cells, as well as the proliferation and development of endothelial capillaries *in vitro*. *In vivo,* Drs B2 also inhibited the growth of a human prostate adenocarcinoma xenograft model that was based on PC-3 cells. Importantly, the experimental analysis of the mode of action against PC-3 cells revealed that Drs B2 targets and disrupts the plasma membrane, resulting in an increase in cytosolic lactate dehydrogenase (independent of the activation of caspase-3), and an increase of the mitochondrial membrane potential. In addition, detailed confocal electron microscopic analysis further revealed the aggregation of Drs B2 on the cell surface and the consequent penetration inside tumor cells, thereby resulting in cancer cell necrosis.

Recent studies on polybia-MPI, an antimicrobial peptide secreted from the venom of the social wasp *Polybia paulista*, demonstrated its antimicrobial activity against both gram-positive and gram-negative bacteria. Polybia-MPI was then synthesized and its antitumor effects on various tumor cell lines were demonstrated; a selective anti-proliferative efficacy and cytotoxicity against bladder and prostate cancer cells via pore formation was observed, with reduced cytotoxicity in normal human murine fibroblasts. To investigate the structure–activity relationship, three variants (Leu^7, Ala^8, and Asp^9) were synthesized, highlighting the importance of the α-helix conformation of MPI in anticancer activity [320].

Additionally, Moore et al. [321] extracted cecropins from the hemolymph of the giant silk moth *Hyalophora cecropia*. *In vitro*,

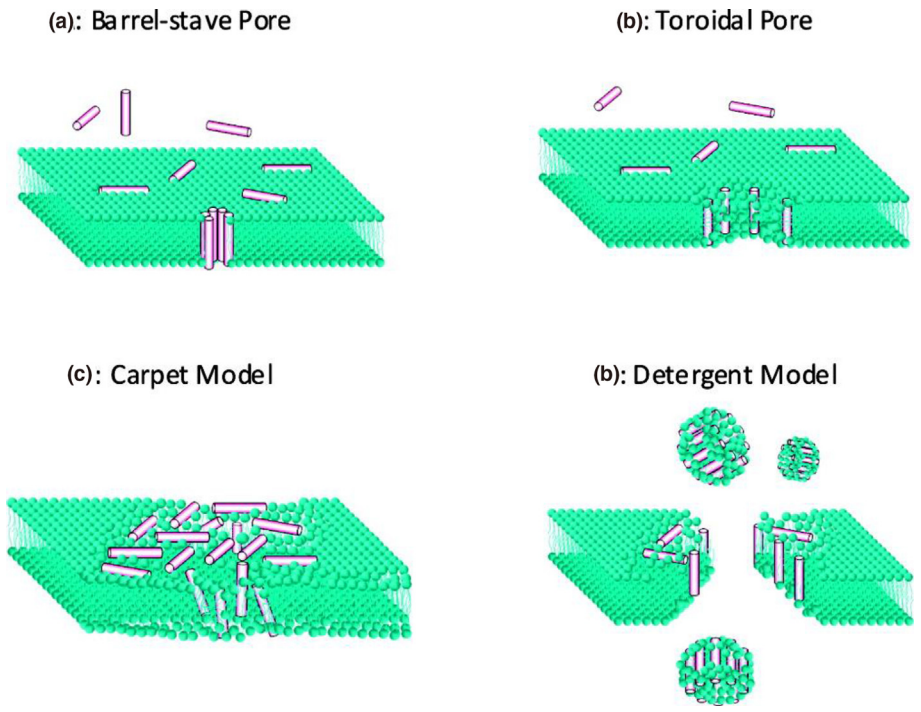

FIGURE 13

Proposed mechanisms for the interactions between ACPs and cancer cells. (a) Barrel-stave model, (b) toroidal pore model, (c) carpet-like mechanism, and (d) detergent-like effect model. Reproduced with permission from Wimley et al. [301], copyright (2010), American Chemical Society.

these peptides showed antibacterial as well as anti-leukemia, and anti-mammalian lymphoma activity. Importantly, different cancer cell lines showed a range of sensitivity to cecropin B (IC_{50} 3.2 to >100 μM), including two multidrug-resistant cell lines that were deemed sensitive to this peptide. Of note, the mode of action is the pore formation at the cytoplasmic membrane.

Apoptotic mechanism. Apoptosis is also a consequence of ACP-induced mitochondrial membrane disruption, which leads to the permeation and swelling of mitochondria and the eventual release of cytochrome-c. Risso et al. [322–324] investigated the BMAP peptides of the cathelicidin family, which are highly cationic in nature. The BMAP-27 and BMAP-28 ACPs, derived from bovine cathelicidin with 27 and 28 amino acid residues, respectively, induced apoptosis in several leukemia cell lines.

Penaeidin-2 (Pen-2), a peptide obtained from the Pacific white shrimp *Penaeus vannamei* with both antibacterial and antifungal activities, was also found to attenuate the growth of A498 and ACHN kidney cancer cells. The mode of action involved the lysis and apoptosis of cancerous cells. Moreover, the MTT assay showed that the maximal growth inhibition of A498, ACHN, and HK-2 cells treated with 100 μg/mL rPen-2 for 48 h was 70.4%, 62.4%, and 13.2%, respectively, suggesting a selectivity toward cancer cells. Of note, fluorescent dye staining also revealed a high percentage of apoptosis in tumor cells [325].

In another study, Kim et al. [326] designed and developed a series of Gaegurin 6 (GGN6) derivatives via the deletion and substitution of amino acids. The authors found that all tested peptides (expect those with the deleted N-terminal region) showed anticancer activity against a series of cancer cell lines. PTP7, which was approximately half the size of GGN6, was the most potent derivative, with antitumor activity analogous to that of GGN6 in a range of multidrug-resistant (MDR) and drug-susceptible human cancer cell lines; importantly, it showed little cytotoxicity against peripheral blood mononuclear and red blood cells.

In addition, Lixiang et al. [327] explored the effects of the bovine lactoferricin P13 (LfcinB-P13) peptide obtained from LfcinB on the human liver cancer cell line SMMC7721 both *in vivo* and *in vitro*. *In vitro*, LfcinB-P13 significantly reduced SMMC7721 cell viability (P = 0.032 vs. untreated cells) and exhibited reduced cytotoxicity to the wild-type liver cell line L02. Additionally, the rate of apoptosis in SMMC7721 cells was significantly enhanced after subsequent treatment with 40 and 60 μg/mL LfcinB-P13 (P = 0.0053 vs. control group) and this correlated with an increase in the ROS levels and the activation of caspase-3 and 9. Importantly, *in vivo*, LfcinB-P13 also inhibited tumor growth in an SMMC7721-xenograft nude mouse model, and thus is a novel therapeutic peptide for the treatment of liver cancer.

Dolastatin 10 is another peptide derived from the marine mollusk *Dolabella auricularia*. *In vitro* cytotoxicity was measured against several human cancer cell lines, such as ovarian cancer, melanoma, colorectal cancer, and sarcoma cancer cells. Interestingly, dolastatin 10 induced apoptosis in various cancer cell lines, via the upregulation of the pro-apoptotic molecule Bax and the downregulation of the anti-apoptotic molecule Bcl-2. [328] Overall, inducing mitochondrial-dependent apoptosis is one of the critical mechanisms underlying the anticancer effects of ACPs.

Angiogenesis inhibition mechanism. Solid tumors are extremely convoluted and formed by neoplastic and neighboring stromal cells. For their growth and dissemination, these tumors require blood

TABLE 7

Membranolytic modes of anticancer peptides.

Model	Membrane lytic mechanism	Peptide	Reference
Barrel-stave model	α-Helices of amphipathic lytic peptides are inserted into the hydrophobic cores of the bilayer membrane and form transmembrane pores	Alamethicin, melittin, and hemolysin	[303,304]
Toroidal or two-state model	Peptides associate with lipid headgroups, which line the inside of the pore with the helical axis parallel to the interface	Magainin	[305]
In-plane diffusion model	Short peptides are inserted in-plane, which disrupts the bilayer packing, reduces membrane thickness, and eventually forms transient pores	Mastoparan and cecropin-melittin hybrids	[304,306,307]
Carpet model	Perpendicular binding of peptides to the membrane in a carpet-like manner via interactions with the lipid head groups of the membrane without insertion into the hydrophobic core	Dermaseptin and magainin	[308,309]
Detergent-like effect model	Disruption of the bilayer by the release of micellar structures from the membrane	Melittin, apolipoproteins, myelin basic protein, and glucagon	[310-313]

vessels and lymphatic vessels as additional conduits for metastatic spread. [329] Therefore, they stimulate vascular endothelial cells to form new blood vessels via high expression levels of the vascular endothelial growth factor (VEGF).

Large plasma proteins are the main source of angiogenesis inhibitors. The Kringle5-like domain (KV) of human apolipoprotein is considered a potential antiangiogenic factor. Yi et al. [330] identified an 11-amino acid long peptide domain (KV11) present in the apolipoprotein as an anti-angiogenesis functional domain. *In vitro*, the authors found that KV11 suppresses the migration of human umbilical vein epithelial cells (HUVECs) and microtubule formation, resulting in the inhibition of angiogenesis. Of note, this ACP showed no effect on HUVECs, and its IC_{50} value was approximately 15 μM. *In vivo*, the KV11 peptide showed no proliferative effect on the tumor cells; however, it significantly prevented the growth of the SCID mouse xenograft tumor model ($P < 0.01$) via the inhibition of angiogenesis.

To identify the angiogenesis inhibitors in microorganisms, Jang et al. [331] extracted the two cyclic peptides PF1171A and PF1171C from the soil fungus *Penicillium* sp. FN070315. *In vitro*, these peptides inhibited the proliferation of HUVECs and were thus considered antiangiogenic. Importantly, both peptides attenuated the VEGF-induced migration, invasion, proliferation, and tubular formation of HUVECs, as well as the neovascularization of the chorioallantoic membrane during the development of chick embryos; the mechanism behind this was the down-regulation of hypoxia-inducible factor-1α and the phosphorylation of VEGF receptor 2.

Overall, the above studies suggest that the mode of action of such peptides is not the direct killing of tumor cells; of note, is that these peptides inhibit neovascularization and thus have minimal side effects on normal cells. Therefore, when compared with traditional drugs, antiangiogenic ACPs are considered better for clinical applications.

Immune regulation mechanism. Immunotherapy is one of the most important cancer therapeutic options [332], as reviewed above. Interestingly, peptides can also be used as immunotherapeutic agents. Zhang et al. [333] examined the stability, cytotoxicity, and internalization of LfcinB and its variants in breast cancer cells. LfcinB (up to 30 μM) inhibited the growth of MDA-MB-231, T-47D, MCF-7, and Hs578T cells to a greater extent than that observed in the context of their normal counterparts (MCF-10-2A cells), indicating their selectivity towards cancer cells. The mode of action was the induction of cytokines that then enhanced the hosts anticancer defenses; in other words, tumor growth was restrained due to immune regulation.

Methionine enkephalin (MENK), an endogenous neuropeptide, plays a major role in the neuroendocrine and immune systems. MENK is involved in the tumor immune response via the upregulation of the activity of $CD8^+$ T cells, and the consequent dendritic cell maturation, intensification of $CD4^+$ T cell functions, and cytokine secretion. Of note, MENK inhibits the expression of the forkhead box P3 transcription factor (FOXP3) during TGF-β induction, thus reducing the levels of regulatory T cells *in vivo* and markedly promoting antitumor effects [334].

Overall, ACPs can boost the immune system through immune-modulatory mechanisms and tumor growth inhibition; however, further investigations are required to fully understand the immune responses in the context of these ACPs. Serial analysis and research on anticancer peptides is essential for the development of new anticancer drugs; however, every method has limitations. ACPs are an expensive cancer treatment, and thus researchers are exploring cationic polymers as an alternative.

Cationic polymeric molecules

Although the above discussed methods showed potent anticancer activities, their clinical usage is limited due to several factors, such as their high manufacturing costs, off-target toxicity, development of drug resistance, and burst release. The limitations of these traditional materials, has led to research into potentially effective systems that use polymers as chemotherapeutic agents.

The negatively charged surface of cancer cells creates possibilities for the development of new drugs. Gakhar et al. [335] reported polymers from three families of cationic, natural, and synthetic. Chitosan and dextran from the polysaccharide family, Lys and Arg-based poly(ester amides) from the amino acid-based poly(ester amides) (AA-PEA) family and polyAETA(2-(acryloxy)ethyl-trimethylammonium chloride) vinyl-based monomers (from the vinyl family) showed different growth inhibitory effects on prostate cancer cells (*versus* normal prostate epithelial

cells - RWPE-1) *in vitro*. The polyAETA (vinyl-based) and Dex-PA (polysaccharide-based) exerted substantial levels of cell toxicity, as <20% of the PC3 cells were viable after being tested with these polymers (Fig. 14). The AA-PEA polymers, however, had no effect when compared to the PBS control group, probably because of the cationic nature of the arginine pendant guanidine group. Of note, it has been reported that free (unconjugated) guanidine has no adverse impact on the growth of bladder cancer cells even at millimolar concentrations [336].

Park et al. [337] designed a macromolecular chemotherapeutic with three principal components: a hydrophilic polyethylene glycol (PEG) block, a linking group, and a cationic block that interacts with the negatively charged lipid membranes. Polycarbonate with pendant benzyl chloride was selected as the cationic block, as it offered an excellent platform from which to introduce the cationic charge and the essential functional groups to enable the polymeric molecules to self-assemble into the micellar structures that are critical for the proposed mechanism. With an improved EPR effect, in theory, the nanoparticles formed will flow through the bloodstream and selectively attack the tumor tissues. Due to the presence of the pH-sensitive linker, the PEG block is expected to be cleaved from the polycarbonate in the tumor tissues (pH 5.8–7.0), allowing the released cationic polycarbonates to interact with the outer cancer cell membrane, causing disruption and subsequent cell lysis (Fig. 15a). Of note, the authors synthesized AB di-block polycarbonate polymers via the organocatalyzed ring-opening polymerization of a benzyl chloride-functionalized cyclic carbonate monomer using hydrophilic PEG as a macroinitiator; the resulting benzyl chloride-functionalized di-block copolymer was then quaternized with a tertiary amine-functionalized cholesterol derivative (Fig. 15b). To balance both the solubility and self-assembly, N,N-dimethylhexylamine was added as a supplementary quaternizing agent. Importantly, the prepared polymers showed self-assembling properties even at low concentrations, with a CMC of 11.4 μg/mL. *In vitro*, the resulting nanoparticles showed high levels of anticancer activity against three human liver carcinoma cell lines, SNU423, Hep3B, and HepG2, with low IC_{50} values. Additionally, *in vivo*, polymer 1c exhibited a significant inhibitory effect on a hepatocellular carcinoma (HCC) patient-derived xenograft (PDX) tumor mouse model as early as 4 days post-treatment (Fig. 15c). The average tumor volumes of the control and polymer 1c-treated groups were 1039 ± 128 mm^3 and 197 ± 78 mm^3, respectively, on day 25 post-treatment. Additionally, the effectiveness of polymer 1c was also tested against cancer stem cells using flow cytometry (Fig. 15d and e). Altogether, this study by Park et al. [337] has demonstrated a new approach for the design of anticancer macromolecular therapeutics that are effective anticancer agents and simultaneously prevent the development of drug resistance.

Zhong et al. [338] synthesized guanidinium-functionalized macromolecular anticancer polymers. A series of triblock copolymers of PEG, guanidinium-functionalized polycarbonate, and polylactide (PEG-PGCm-PLAn) were prepared using organocatalytic ring-opening polymerization (OROP) (Fig. 16a and b). This combination, along with the polylactide block was designed assuming that polylactide stimulated the polymers to self-assemble into micelles via hydrophobic interactions, shielding the cationic polycarbonate from enzymatic degradation, and thus improving its stability *in vivo*. Of note, micelles formed from a smaller anticancer PGC block that showed higher CMC values because of the increased hydrophilicity of the longer PGC block. The cytotoxicity of these polymers was tested on different cancer cell lines (BCap37, HepG2, A549, and A431), including MDR cells *in vitro*; their selectivity was estimated using normal human cell lines (a human hepatic HL-7702 cell line and primary human dermal fibroblasts). Importantly, the block polymers demonstrated broad-spectrum anticancer activity. Interestingly, the IC_{50} values were below the polymers' CMCs, suggesting that micelle formation is not required for anticancer activity. In fact, an increase in the PGC block increased the anticancer activity and reduced the IC_{50} values in the context of all cancer cell lines due to the increase in the number of guanidinium groups and the expected increase in the interactions with the cancer cell membranes. Importantly, the polymers also showed efficacy *in vivo*, in a metastatic 4T1 subcutaneous tumor model; a decrease in the size of metastasized lesions was observed in the lung tissues of the polymer-treated groups, attesting to the capability of the micelles to inhibit distant metastasis (Fig. 16c and d). Overall, these results suggest that these easily synthesizable polymers, which are not associated with resistance, are promising candidates for future macromolecular cancer therapeutics.

Based on this membrane-targeting mechanism, Takahashi et al. [339] published a report on the design of a new class of anticancer polymers. The authors designed and synthesized a series of new anticancer cationic polymers inspired by membrane-active host defense peptides, that were effective in killing dormant prostate cancer (PCa) cells (Fig. 17a and b) [340–342]. The polymers showed a low molecular weight along with a random sequence of the monomers, with both cationic and hydrophobic side chains. Of note, it is assumed that cationic and hydrophobic properties are essential functionalities and the minimum requirements for establishing membrane-targeting anticancer selective agents. Interestingly, the authors also prepared methacrylate random copolymers with an ammonium group as the cationic side chain, which binds to anionic phosphatidylserine lipids via electrostatic interactions. The molecular weight of these polymers was 2000–3000 g/mol with a relatively narrow polydispersity (1.1–1.3); importantly, they were highly soluble in both water and cell culture media. Importantly, *in vitro*, these copolymers were cytotoxic in a concentration-dependent manner to three metastatic PCa cell lines (PC-3, DU145, and C4-2B cells) associated with bone tropism and brain metastasis; of note, 100% toxicity was recorded for polymer concentrations (Fig. 17c and d).

Cancer can also be treated using antibiotics owing to their anti-proliferative and cytotoxic properties. However, antitumor antibiotics such as doxorubicin, paclitaxel, and ciprofloxacin have limitations. Their effective concentrations exceed the pharmacological range, which may result in severe toxicity to the liver, skin, central nervous system, gastrointestinal tract, and urinary tract [343,344]. Additionally, drug resistance frequently emerges [345,346]. To overcome such limitations, Zheng et al. [347] devised a combination therapy in which ammonium-functionalized polycarbonates are used along with re-purposed antibiotics for the treatment of cancer; the authors explored

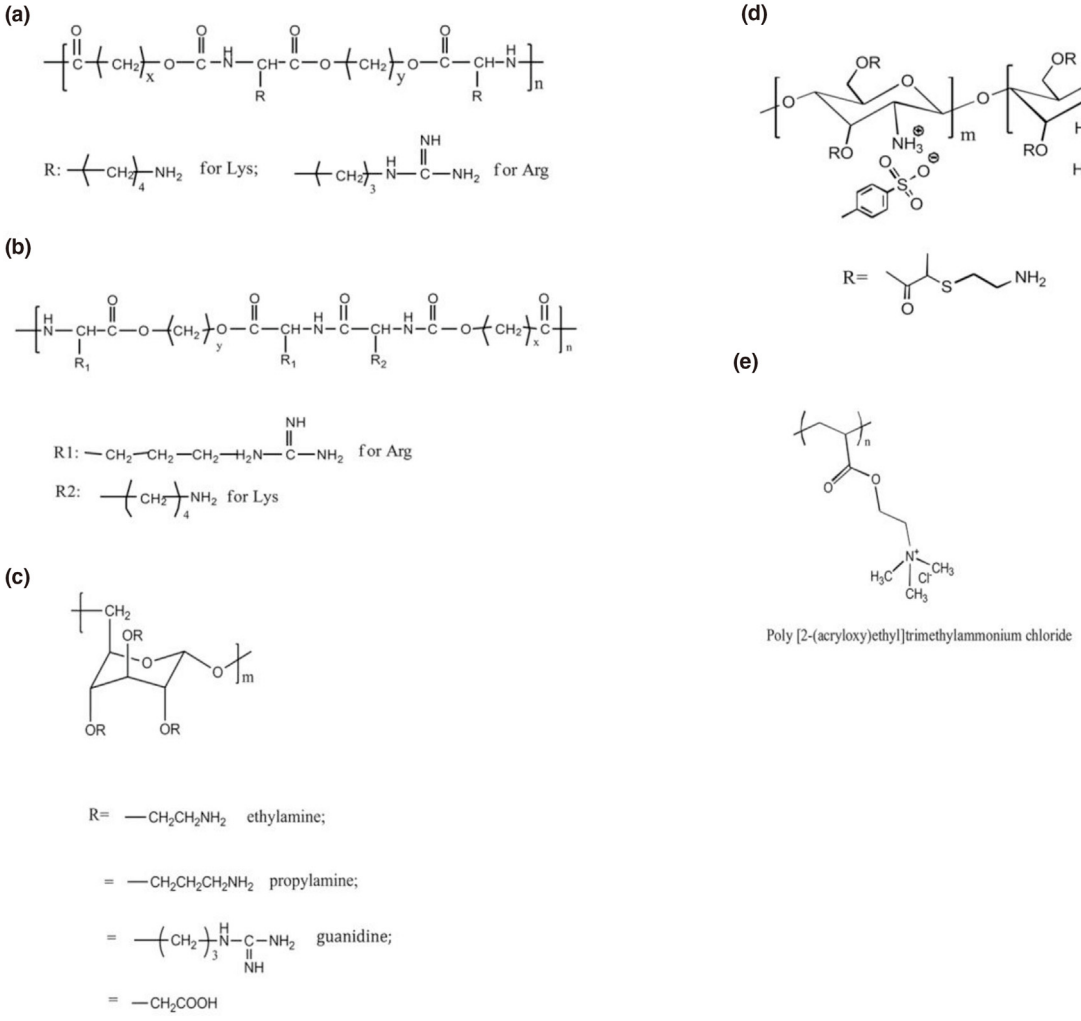

FIGURE 14

Different cationic polymeric molecules. (a) Amino acid-based cationic poly (ester amides), (b) multi-amino acid-based poly (ester amides), (c) dextran based cationic polymers, (d) GMA-chitosan-NH_2 based polymers, and (e) poly AETA-based cationic vinyl polymers. Reproduced with permission from Gakhar et al. [335], copyright (2014), International Institute of Anticancer Research.

the effect of cationic polymers in synergy with doxorubicin, paclitaxel, and antitumor antibiotics in various types of cancer cells, especially in drug-resistant cell lines. From a mechanistic point of view, these quaternary ammonium-functionalized polymers damaged the cell membrane, increasing drug uptake even in drug-resistant cell lines, and consequently counteracting the effects of drug efflux and restoring drug susceptibility. These findings expand the use of cationic polymers for the selective and effective treatment of cancer.

Additionally, in a recent work, Zhou et al. [348] demonstrated the synergistic effects of photothermal and photodynamic therapies when using a conjugated polymers with a cationic side chain (PTDBD). The backbone of the polymer was developed using a donor–acceptor (D-A) strategy via the incorporation of electron-rich and electron-deficient moieties (Fig. 18a); as a result, the polymer shows an intense absorbance at wavelengths of 600–1000 nm, which falls within the therapeutic window. Importantly, the authors demonstrated that upon irradiation with a NIR light, these conjugated polymers not only produced heat (Fig. 18b) but also generated ROS (Fig. 18c), leading to a cytotoxic synergy against cancer cells *in vitro* (Fig. 18d) and *in vivo*, in mouse xenografts (Fig. 18e). These findings highlight that completely synthetic polymers can also eliminate tumors, and are, therefore promising alternatives as photo-agents for tumor therapy in clinical practice.

Bacteria-assisted therapy

An anticancer approach that is of increasing interest is bacteria-assisted cancer therapy. This strategy involves the direct injection of bacteria into the target site for anticancer purposes. Bacterial therapy offers unique advantages such as high specificity, the possibility of genetic engineering to meet specific requirements, and it does not use toxic chemical agents [349]. William Coley was perhaps one of the first researchers to use bacteria therapy for the treatment of cancer, and noted that in some patients, the presence of bacterial infection triggered the elimination of malignant tumors [350,351]. Of note, tumors are often devoid of oxygen (contrary to all organs in the human body), thus providing an optimum environment for obligate anaerobes to grow in a tumor-specific fashion [352,353]. Multiple studies

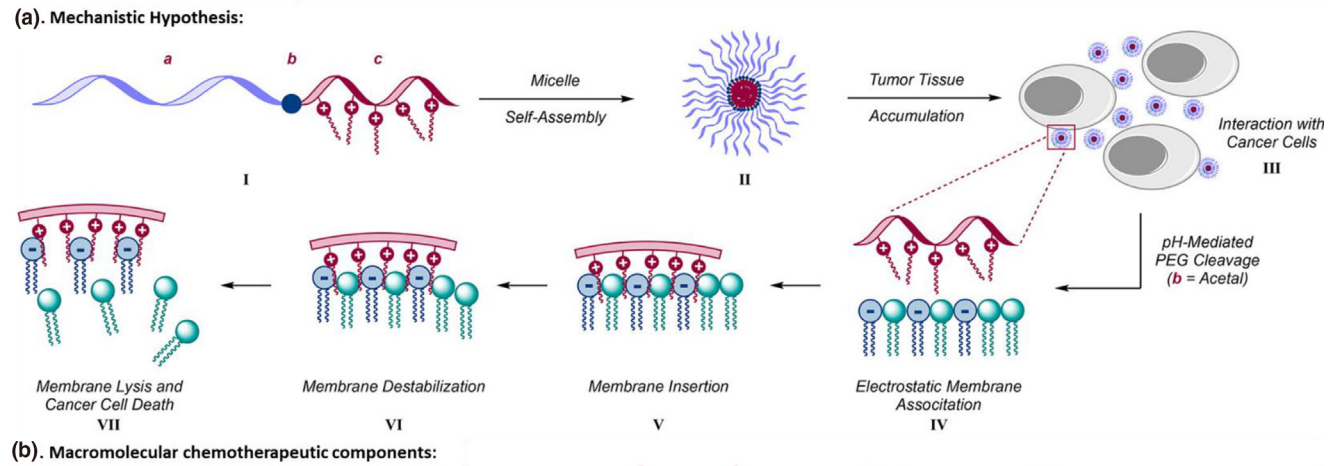

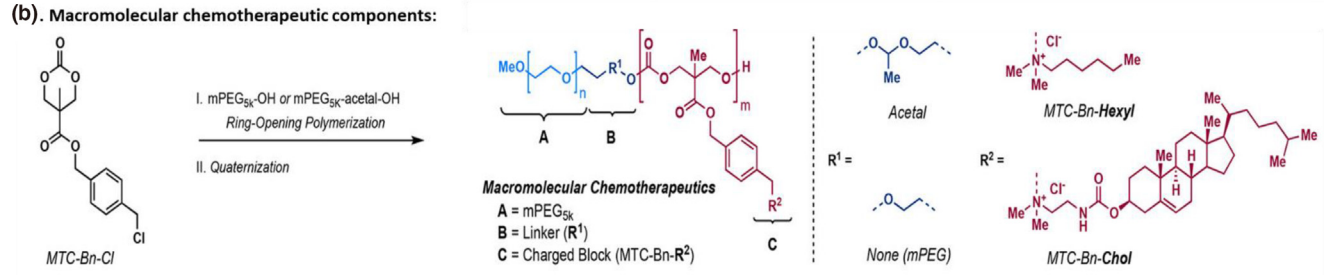

Entry	Polymer	Composition	CMC (μg/mL)	Size (nm)	PDI	ZP (mV)
1	**1a**	$mPEG_{5K}$-p[MTC-Bn-Chol]$_{10}$	7.5	55.8 ± 0.6	0.37 ± 0.02	0.9 ± 0.4
2	**1b**	$mPEG_{5K}$-acetal-p[MTC-Bn-Chol]$_{10}$	7.8	88.9 ± 2.6	0.30 ± 0.02	1.4 ± 0.5
3	**1c**	$mPEG_{5K}$-p[(MTC-Bn-Chol)$_8$-(MTC-Bn-Hexyl)$_3$]	11.4	23.2 ± 0.2	0.13± 0.02	1.5 ± 1.1
4	**1d**	$mPEG_{5K}$-acetal-p[(MTC-Bn-Chol)$_8$-(MTC-Bn-Hexyl)$_{3.4}$]	12.2	74.4 ± 0.3	0.22 ± 0.01	4.6 ± 1.3
5	**1e**	$mPEG_{5K}$-p[(MTC-Bn-Chol)$_4$-(MTC-Bn-Hexyl)$_{3.5}$]	13.5	53.3 ± 0.3	0.18 ± 0.01	1.4 ± 0.2
6	**1f**	$mPEG_{5K}$-acetal-p[(MTC-Bn-Chol)$_4$-(MTC-Bn-Hexyl)$_{3.5}$]	17.3	106.2 ± 0.8	0.21 ± 0.01	0.9 ± 0.3

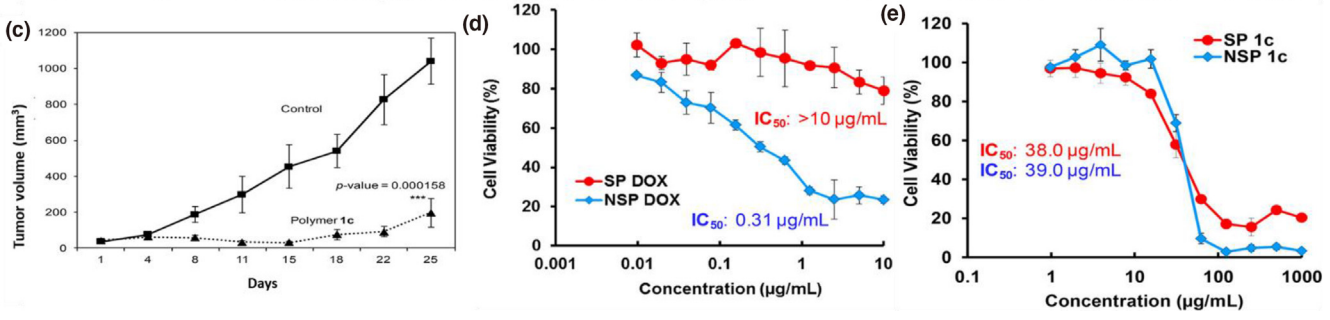

FIGURE 15

Macromolecular chemotherapeutic. (a) Mode of action of the cationic polymers. (b) Scheme for the synthesis of the diblock co-polymer. (c) Measurement of the tumor volume (mm^3) in both the control and polymer 1c groups to determine anticancer efficacy in a human HCC PDX xenograft mouse model with patient-derived tumors. (d) Effectiveness of doxorubicin in Hep3B cancer stem cell (SP) lines and non-cancer stem cells (NSP). (e) The activity of polymer 1c in Hep3B cancer stem cell (SP) lines and non-cancer stem cells (NSP). Reproduced with permission from Park et al. [337], copyright (2018), American Chemical Society.

have been conducted using bacterial therapy in both animal models [354–357] and human trials [358–360], with good efficiency.

Zheng et al. [361] combined a photocatalyst system with tumor-targeting bacteria via the assembly of carbon-dot doped carbon nitride and *E. coli* through electrostatic interactions, and consequently developed a photo-controlled bacterial metabolite therapy (PMT). They demonstrated that this therapy metabolized NO_3^- to cytotoxic NO upon irradiation with red light (>630 nm, 30 mW cm^{-2}). While Chen et al. [362] covalently attached the surface of a genetically-modified *Salmonella typhimurium* strain (YB1) to ICG to obtain a biotic/abiotic cross-linked system (YB1-INPs) (Fig. 19). With photothermal therapy, this system was found to accumulate more in the tumor region

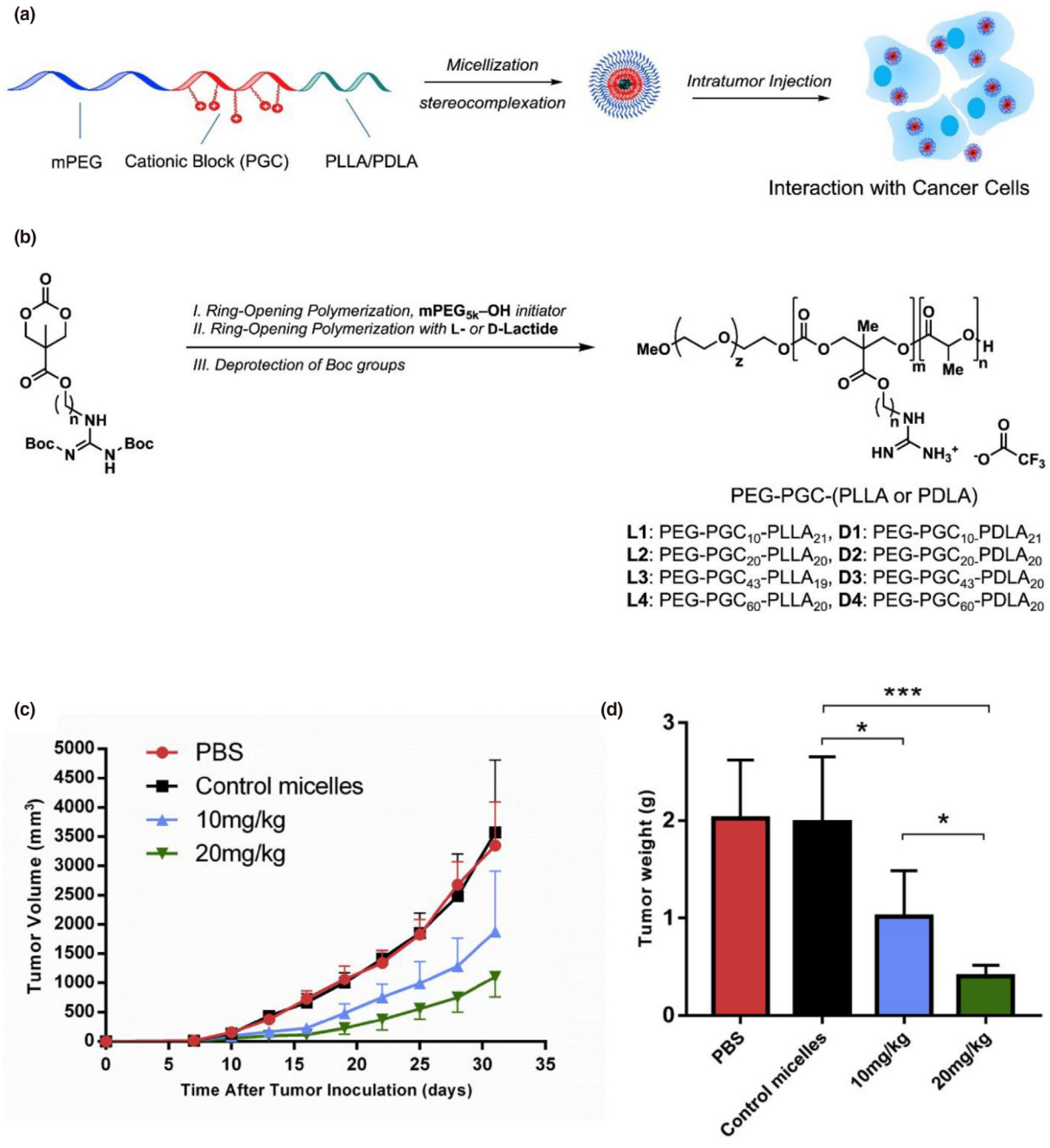

FIGURE 16

Guanidinium-functionalized macromolecular anticancer polymers. (a) Mechanistic hypothesis. (b) Scheme of the guanidinium-functionalized PEG-PGCm-PLAn triblock copolymers that can self-assemble. (c) Change in the tumor volume over time after treatment with PBS, control micelles, or L3/D3 at 10 or 20 mg/kg mouse body weight. (d) Change in the tumor weight over time after treatment with PBS, control micelles, or L3/D3 at 10 or 20 mg/kg mouse body weight. Reproduced with permission from Zhong et al. [338], copyright (2019), Elsevier.

(*versus* no photothermal treatment). In fact, upon irradiation with a NIR laser, YB1-INPs exhibited remarkable efficiency in the removal of large tumors.

Additionally, in a study by Yang et al. [363], purple photosynthetic bacteria (PPSB; *Rhodopseudomonas palustris* and *Blastochloris viridis* as models) with light-harvesting nanocomplexes were employed in cancer theranostics. The authors used a NIR laser in combination with PPSB to achieve high photothermal conversions as well as the generation of ROS and contrasting photoacoustic effects. Upon irradiation with the NIR laser, *R. palustris* showed greater toxicity to cancer cells than to non-irradiated cells (Fig. 20a and 20b), demonstrating the ability of these systems to eliminate cancer cells. Of note, the *in situ* injection of PSSB and subsequent NIR irradiation led to efficient tumor eradication (Fig. 20c and d). Moreover, macrophages were found at the tumor sites, and the expression of macrophage-associated markers decreased after treatment with the laser-induced *R. palustris*, suggesting that the strong photothermal effect and ROS-generating capability of *R. palustris* were induced by the laser irradiation.

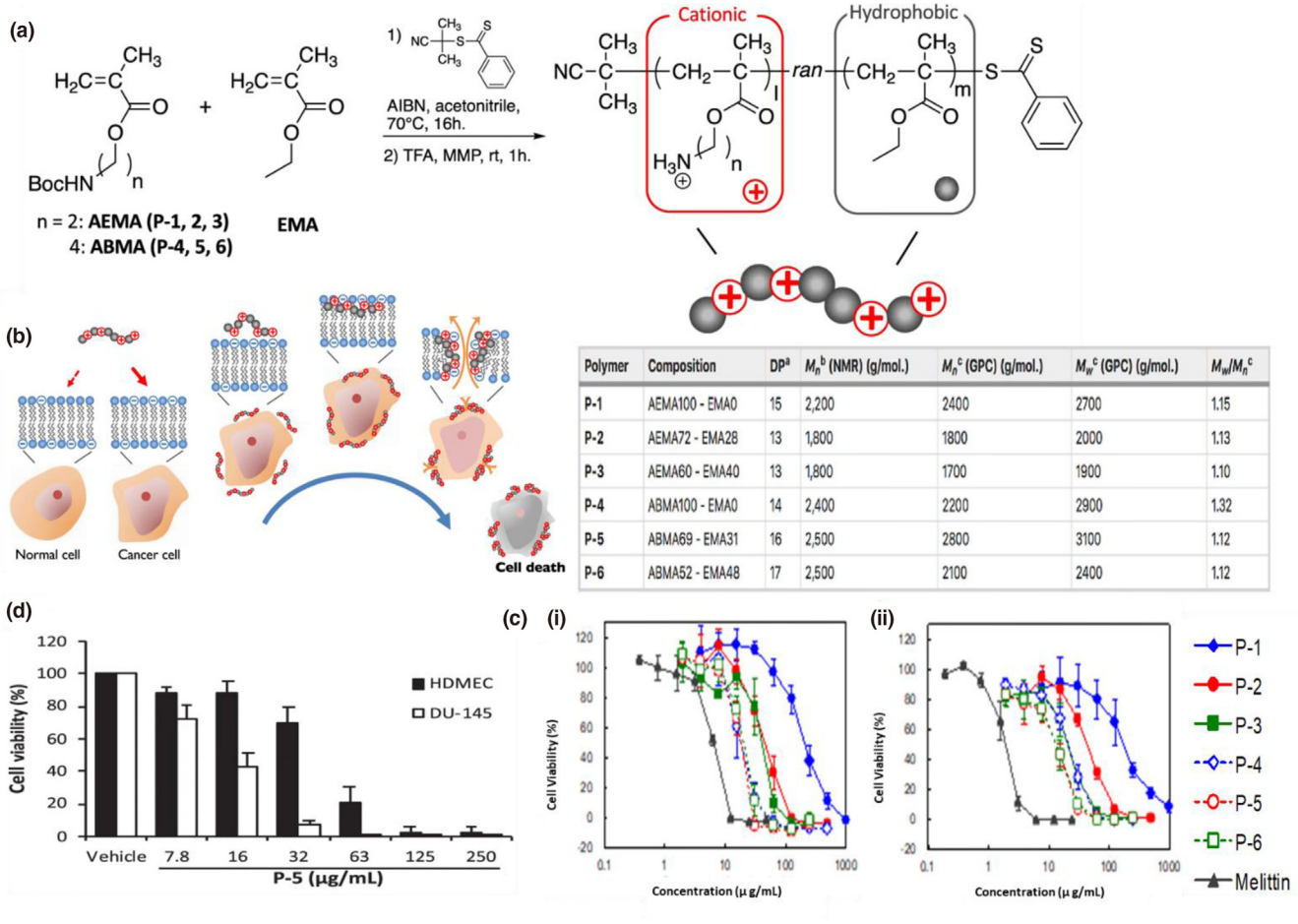

Polymer	Composition	DP[a]	M_n[b] (NMR) (g/mol.)	M_n[c] (GPC) (g/mol.)	M_w[c] (GPC) (g/mol.)	M_w/M_n[c]
P-1	AEMA100 - EMA0	15	2,200	2400	2700	1.15
P-2	AEMA72 - EMA28	13	1,800	1800	2000	1.13
P-3	AEMA60 - EMA40	13	1,800	1700	1900	1.10
P-4	ABMA100 - EMA0	14	2,400	2200	2900	1.32
P-5	ABMA69 - EMA31	16	2,500	2800	3100	1.12
P-6	ABMA52 - EMA48	17	2,500	2100	2400	1.12

FIGURE 17

Anticancer cationic polymers. (a) Scheme for the synthesis of different polymers. (b) Proposed mechanism of anticancer activity. (c) Viability of C4-2B (a), DU145 (b), cells after being treated with polymers and melittin for 24 h. (d) Cytotoxicity of polymer P-5 against human dermal microvascular endothelial cells (HDMECs) and DU-145 cells. Reproduced with permission from Takahashi et al. [339], under the creative common's attribution 4.0.

Magnetotactic bacteria (MTB) have also been routinely employed for cancer immunotherapy. These bacteria have magnetosomes that act as a compass for their orientation along the earth's magnetic field and are believed to possess the ability of aerotaxis (migration in function of the oxygen concentration) [364]; they are often used as nanobots, as they can be externally guided by magnetic fields and have a tendency to accumulate in hypoxic regions. They have also been frequently used as carriers of anti-cancer drugs due to their capacity for targeted administration [365,366]. Importantly, MTBs can act as magnetic hyperthermia agents due to the presence of iron-rich magnetic particles, increasing the temperature of cancer cells and leading to apoptosis. Interestingly, Gandia et al. [367] in a recent study explored the use of whole magnetotactic bacteria as hyperthermia agents for the treatment of cancer and observed that cancer cell proliferation was affected by the administration of the MTBs, thus demonstrating their immense potential as nanobots in cancer treatments.

Importantly, bacteria-assisted therapy is a very promising anti-cancer strategy, that could be utilized with individualized therapy programs. Although further research is required to investigate some of the minor shortcomings such as genetic instability and targeting efficiency as well as the ethical concerns regarding genetic manipulation and the risks of virulent revertants involved with genetic manipulation [368]. It is believed that this technology has the potential to change the landscape of anticancer therapy, with significantly higher efficiencies than those of conventional therapies. Representative bacterial cancer therapies that have been applied in combination with functional nanomaterials are summarized in Table 8.

Conclusions and future perspectives

As the world gradually recovers from a global pandemic, it is imperative that we look for innovative ways to prevent new disorders and to treat existing diseases. Cancer has been one of the biggest challenges faced by humanity in the preceding centuries; therefore, combating this disease(s) should be a top priority for researchers and lawmakers globally. It must be noted that cancer does not only exerts physical strain but also has a financial and emotional impact on individuals, families, communities, and health care systems. A large amount of work has been done in cancer research, with numerous groundbreaking reports published. Many existing cancer therapies have become more effi-

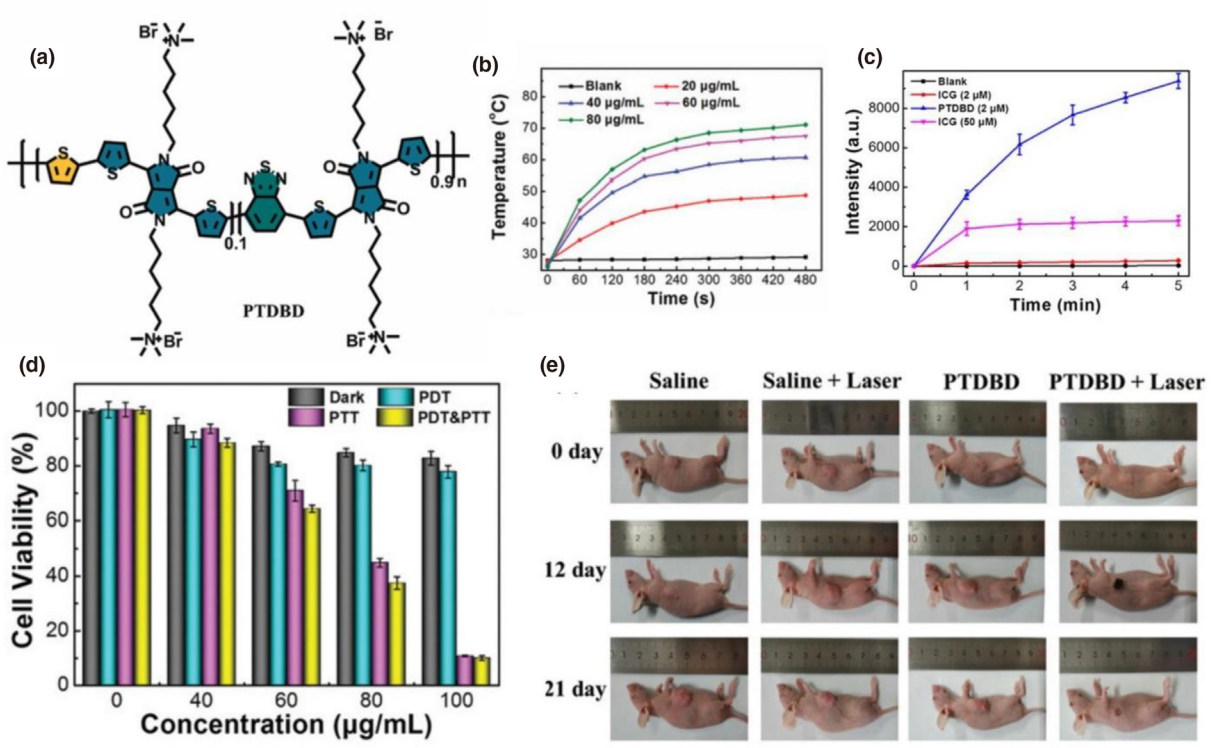

FIGURE 18

Antitumor effects of water-soluble conjugated polymers. (a) Chemical structure of PTDBD, enriched with electron-deficient benzothiadiazole and diketopyrrolopyrrole and electron-rich thiophene. (b) Photothermal activity of PTDBD upon NIR irradiation. (c) ROS generation with PTDBD and ICG. (d) Cell viability of HeLa cells treated with different polymer concentrations and different interventions. (e) Images of tumor-induced mice after the injection of PTDBD. Reproduced with permission from Zhou et al. [348], copyright (2019), Royal Society of Chemistry.

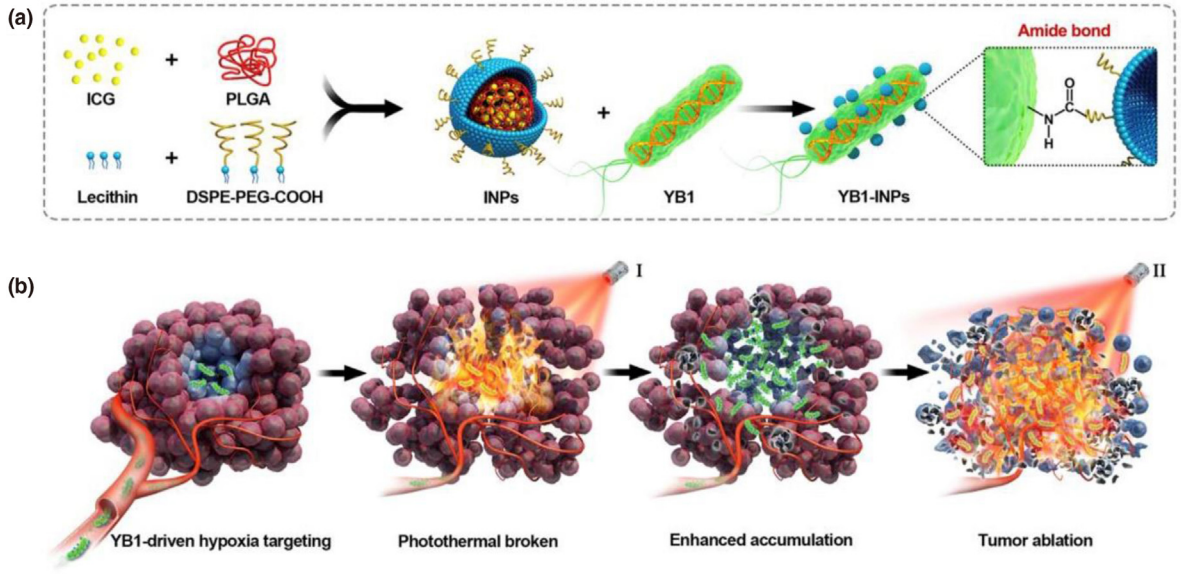

FIGURE 19

Novel YB1-INPs. (a) The strategy used for the development of YB1-INPs. (b) The hypoxia-targeting activity of YB1-INPs, with tumor ablation effects. Reproduced with permission from Chen et al. [362], copyright (2019), Elsevier.

cient and reliable with time, while newer technologies and chemical compounds have become more established and proven to be extremely effective.

While the removal of tumors via surgery, radiation-based killing of cancerous cells, and chemotherapy have proven to be game-changers in the field of cancer treatments, numerous issues

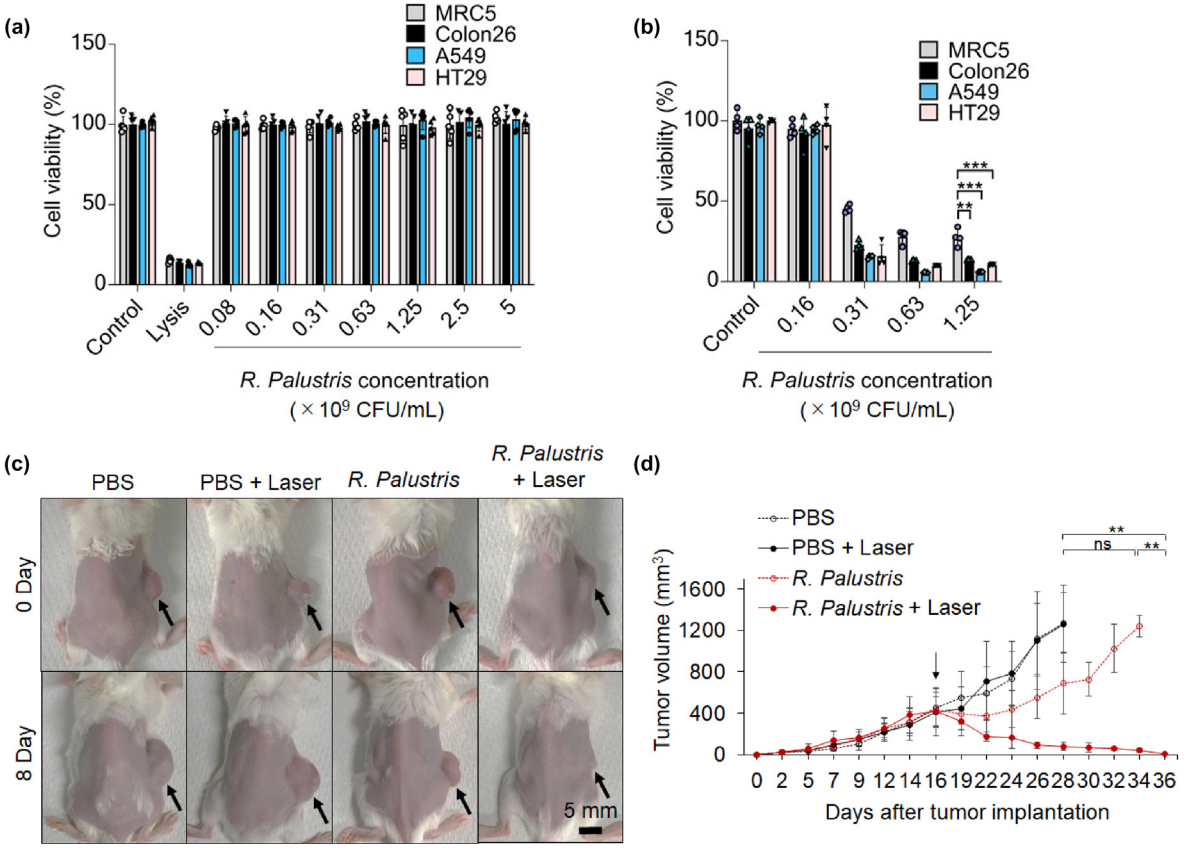

FIGURE 20

Cancer treatments using purple photosynthetic bacteria. (a, b) Cytotoxicity of *R. palustris* against various cancer cell lines at various bacterial concentrations without (a) and with (b) NIR irradiation; laser power = 1.2 W (ca. 61.1 mW/mm^2); irradiation time = 5 min. (c) Images of a tumor xenograft mouse model after treatment with *R. palustris* or PBS with and without laser treatment. (d) Change in the tumor volume after each treatment. Reproduced with permission from Yang et al. [363], copyright (2021), Elsevier.

have been raised challenging the development of effective therapeutic regimens. Aggressive drug resistance is believed to be one of the most problematic concerns with current treatments. Additionally, the low aqueous solubility of many chemotherapeutic drugs, insufficient drug accumulation, rapid clearance from the body, and significant off-target toxicity are also responsible for ineffective outcomes. Moreover, cancer treatments involving radiation, chemotherapy, and surgery may harm the normal functions of the surrounding cells.

As an alternative to the above approaches, nanotechnology-based drug delivery treatment options can combine different treatment modalities, drugs, and materials in a single platform. Nanoparticle-based medicines possess several unique properties that make them attractive for drug delivery and cancer therapy; for instance, drug loading into nanoparticles alters the drug pharmacokinetic properties, prevents drug degradation inside the body, and reduces drug toxicity and side effects. Unfortunately, nanoparticle drug delivery systems are based on the activity of the drug itself and hence are still associated with the limitations inherent for the drug. Although the concentration of chemotherapeutic drugs can be increased in tumor tissues with these systems, cellular barriers and resistance mechanisms still limit drug effectiveness. Burst release, significant off-target toxicity, loading issues of several small molecules (chemosensitizing agents), and material-related limitations are other drawbacks of these systems. However, we are convinced that further research into the use of the many different types of nanoparticles for biomedical applications and the complete understanding of the interplay between their physicochemical and the biological properties of tumors will ultimately pave the way for the development of smart drug delivery systems in the future.

Importantly, anticancer peptides have also been proven as selective and potent agents for the treatment of cancer. Both natural and synthetic candidates have been derived, synthesized, and developed as novel candidates against various cancer types. A few ACPs have shown apoptotic and anti-proliferative activity in various cancer cell types, both *in vitro* and *in vivo*. In fact, several ACPs are undergoing clinical trials in relation to cancer treatment and vaccine development. Nevertheless, there are some notable disadvantages associated with the use of ACPs, such as low bioavailability, biological instability, protease sensitivity, short half-life, first-pass metabolism, and poor pharmacokinetics. Apart from the low selectivity, high production cost on a large scale, and lower resistance towards proteolytic cleavage are some reasons for researchers to look for other alternatives.

In contrast to anticancer peptides, research on anticancer polymers is comparatively new. However, these cationic polymeric macromolecules have shown great promise. They were

TABLE 8

Bacterial cancer therapies applied in combination with functional nanomaterials.

Therapeutic approach	Bacteria	Biomaterial	Remarks	Reference
PTT and photodynamic therapy (PDT)	*Rhodopseudomonas palustris* or *Blastochloris viridis*	Light-harvesting nanocomplexes in natural *Rhodopseudomonas palustris* or *Blastochloris viridis*	Light-driven bacterial multifunction allows effective tumor targeting immunological regression	[363]
PTT	*Salmonella enterica serovar Typhimurium* strain VNP20009	Polydopamine coating on bacterial surface	Effective anti-metastatic response	[369]
	Bifidobacterium breve and/or *Clostridium difficile*	Au nanoparticle	Synergetic targeting for tumor ablation	[370]
	Salmonella Typhimurium strain YB1	ICG-loaded poly(lactic-co-glycolic acid) nanoparticle	Effective tumor ablation	[362]
PDT	*Synechococcus elongatus* strain PCC 7942	ICG-encapsulated human serum albumin nanoparticles	Photocatalyzed oxygen generation with cyanobacteria allows immunogenic PDT	[371]
		PEG-modified photosensitizer chlorin e6	Photosynthesis enhanced photodynamics	[372]
PMT	*Escherichia coli*	Carbon nitride semiconductor nanoparticle	Light-driven metabolic reactions generate cytotoxic NO to eliminate cancer cells	[361]
Magnetic hyperthermia	*Magnetospirillum gryphiswaldense* strain MSR-1	Magnetic nanoparticle in natural MSR-1 cell	*In vitro* studies under a magnetic field	[367]
Chemotherapy	*Magnetococcus marinus* strain MC-1	Anticancer drug (SN-38)-loaded liposome	Magnetic field assists in tumor targeting	[364]
	Salmonella enterica serovar Typhimurium strain VNP20009	Anticancer drug (hydroxychloroquine)-encapsulated liposome	Effective anticancer response	[373]
		Fluorophore 6,13-bis (triisopropylsylylethynyl) pentacene-loaded poly(lactic-co-glycolic acid) nanoparticle	Effective tumor targeting effect	[374]
		Plasmid DNA polyplex nanoparticle	Oral vaccination	[375]

deemed effective and selective against various cancer cell lines, including multidrug-resistant cancer cells, inhibiting tumor metastasis, and suppressing tumor growth both *in vivo* and *in vitro*. Overall, synthetic cationic polymers provide a simple but novel platform that allows the tuning of the physiological properties and the consequent improvement of cytotoxicity and selectivity towards cancer cells. Although further targeted research is required, we believe that these cationic platforms will allow for the rational design and screening of functional degradable polymers. Polymer architectures and morphologies (e.g., polymer micelles) can also be obtained, and chemical modifications, including the inclusion of cancer-homing ligand groups or prodrug moieties can be performed, which will ultimately lead to the development of clinically potent selective compounds.

Even though advancements in material science and nanotechnology have led to the establishment of different therapeutic modalities for cancer treatment as highlighted in this review, the therapeutic strategies currently employed in the clinics are still far from ideal. This is due to the highly heterogeneous nature of cancer, which makes it difficult to strategize and obtain a desired therapeutic outcome using a specific treatment modality. The clinical translation of therapeutic strategies faces a lot of challenges such as difficulties in large scale manufacturing, tumor metastases, and immune effects. Additionally, there are not enough tumor models that can perfectly replicate all the characteristics of human cancer, which leads to the failure of therapies at the clinical stages even after successful *in vitro* and *in vivo* studies in research laboratories [376,377]. Furthermore, it has been observed that the absence of defined regulatory or safety criteria from government agencies has also mitigated clinical translation, especially for newer methods like those using polymeric systems [378]. To address this major limitation, present and future therapeutic techniques developed for the treatment of cancer should be based on combination strategies including various stimuli-responsive or image-guided drug delivery systems. Using such multi-functional/combination techniques, a personalized approach for the treatment of cancer can be made possible in the future. Furthermore, expanding our understanding of tumor biology, including the tumor EPR, cell population heterogeneity, tumor-immune system interactions, invasion, and metastatic behavior is essential to support the development of more specific treatment modalities. Moreover, further research is warranted to optimize selectivity against cancer cells/tumors (*versus* normal cells/nearby organs), which is currently a major issue in the field of cancer treatment. With the advent of new materials and technologies, the next few decades are expected to radically change the way cancer is understood and treated.

Data availability

Data can be requested from the corresponding authors upon reasonable request.

CRediT authorship contribution statement

Nishant Kumar: Writing – original draft, Writing - review & editing. **Sajid Fazal:** Writing – original draft, Writing - review & editing. **Eijiro Miyako:** Writing - review & editing, Supervision, Funding acquisition. **Kazuaki Matsumura:** Supervision, Project administration, Conceptualization. **Robin Rajan:** Writing - review & editing, Supervision, Project administration, Conceptualization.

Declaration of Competing Interest

The authors declare that they have no known competing financial interests or personal relationships that could have appeared to influence the work reported in this paper.

Acknowledgements

We would like to thank Editage (www.editage.com) for English language editing.

Funding

This work was supported by the Japan Society for the Promotion of Science (JSPS) KAKENHI Grant-in-Aid for Scientific Research (A) [grant number 19H00857 to E.M.].

References

[1] World Health Organisation, Cancer. (2021).
[2] W.H. Yoon et al., Biochem. Biophys. Res. Commun. 222 (3) (1996) 694.
[3] M.D. Burdick et al., J. Biol. Chem. 272 (39) (1997) 24198.
[4] H.S. Lee et al., Cancer Lett. 271 (1) (2008) 47.
[5] J. Kleeff et al., J. Clin. Invest. 102 (9) (1998) 1662.
[6] D.W. Hoskin, A. Ramamoorthy, Biochim. Biophys. Acta 1778 (2) (2008) 357.
[7] S.C. Chan et al., Anticancer Res. 18 (6a) (1998) 4467.
[8] O. Warburg, Science 123 (3191) (1956) 309.
[9] V. Bhardwaj et al., Anticancer Res. 30 (3) (2010) 743.
[10] B. Chen et al., Theranostics 6 (11) (2016) 1887.
[11] M. Xie et al., Open Biol. 10 (7) (2020) 200004.
[12] H.H.W. Chen, M.T. Kuo, Oncotarget 8 (37) (2017) 62742.
[13] C.Y. Huang et al., Biomedicine (Taipei) 7 (4) (2017) 23.
[14] J. Tan et al., Biomaterials 252 (2020) 120078.
[15] J.H. Breasted, The Edwin Smith Surgical Papyrus, University of Chicago Press,:, 1930.
[16] S.I. Hajdu, Cancer 100 (10) (2004) 2048.
[17] A. Castiglioni, Histoire de la Medecine (1931).
[18] I.S. Dayes et al., Curr. Oncol. 13 (4) (2006) 124.
[19] R. Rajan, K. Matsumura, Development and application of cryoprotectants, in: M. Iwaya-Inoue (Ed.), Survival Strategies in Extreme Cold and Desiccation: Adaptation Mechanisms and Their Applications, Singapore, Springer Singapore, 2018, p. 339.
[20] T. Wirth et al., Gene 525 (2) (2013) 162.
[21] T. Li et al., Oncol. Lett. 16 (1) (2018) 687.
[22] D. Killock, Nat. Rev. Clin. Oncol. 17 (7) (2020) 391.
[23] J.R. Gregg, T.C. Thompson, Nat. Rev. Urol. 18 (3) (2021) 170.
[24] B.R. Webster et al., Curr. Probl. Cancer 45 (4) (2021) 100773.
[25] G. Giamas, Cancer Gene Ther. 27 (3–4) (2020) 115.
[26] P.M. Glassman, V.R. Muzykantov, J. Pharmacol. Exp. Ther. 370 (3) (2019) 570.
[27] H. Wang et al., Nanomedicine (Lond) 11 (2) (2016) 103.
[28] M.J. Ernsting et al., J. Control. Release 172 (3) (2013) 782.
[29] V. Torchilin, Adv. Drug Deliv. Rev. 63 (3) (2011) 131.
[30] W. Hasan et al., Nano Lett. 12 (1) (2012) 287.
[31] Q. Hu et al., Biomaterials 34 (22) (2013) 5640.
[32] Q. Pan et al., ACS Biomater. Sci. Eng. 6 (4) (2020) 2175.
[33] M.S. Strand et al., Oncotarget 10 (46) (2019) 4761.
[34] S. Wohlfart et al., PLoS ONE 6 (5) (2011) e19121.
[35] C. Song et al., J. Mater. Chem. B 8 (14) (2020) 2768.
[36] C.M. Patterson et al., Commun. Biol. 4 (1) (2021) 112.
[37] L.M. Kaminskas et al., Nanomedicine 8 (1) (2012) 103.
[38] Y. Dong et al., J. Am. Chem. Soc. 140 (47) (2018) 16264.
[39] Y. Cui et al., ACS Appl. Mater. Interfaces 8 (3) (2016) 2193.
[40] Y. Zhang et al., Int. J. Nanomed. 11 (2016) 1119.
[41] E.K. Park et al., J. Control. Release 109 (1–3) (2005) 158.
[42] Y. Li et al., BMC Cancer 14 (2014) 329.
[43] M. Alibolandi et al., J. Control. Release 241 (2016) 45.
[44] D. Zhu et al., Acta Biomater. 75 (2018) 386.
[45] X. Yang et al., ACS Nano 4 (11) (2010) 6805.
[46] Y. Du et al., Biomaterials 33 (29) (2012) 7291.
[47] W.H. Chiang et al., Langmuir 28 (42) (2012) 15056.
[48] S.S. Desale et al., J. Control. Release 208 (2015) 59.
[49] Z.Y. Qiao et al., J. Control. Release 152 (1) (2011) 57.
[50] D. Maciel et al., Biomacromolecules 14 (9) (2013) 3140.
[51] R.M. Schiffelers et al., J. Control. Release 91 (1–2) (2003) 115.
[52] K.M. Camacho et al., J. Control. Release 229 (2016) 154.
[53] L. Battaglia et al., Nanomedicine (Lond) 12 (6) (2017) 639.
[54] R. Rosiere et al., Mol. Pharm. 15 (3) (2018) 899.
[55] J.H. Kim et al., Mol. Pharm. 12 (4) (2015) 1230.
[56] S. Jaraswekin et al., J. Microencapsul. 24 (2) (2007) 117.
[57] J.S. Winkler et al., Exp. Biol. Med. (Maywood) 244 (14) (2019) 1162.
[58] B. Surnar et al., Nanoscale 7 (42) (2015) 17964.
[59] J. Kopecek, P. Kopeckova, Adv. Drug Deliv. Rev. 62 (2) (2010) 122.
[60] H. Dozono et al., Target Oncol 11 (1) (2016) 101.
[61] T.X. Viegas et al., Bioconjug. Chem. 22 (5) (2011) 976.
[62] L.P. Wu et al., Bioconjug. Chem. 26 (7) (2015) 1198.
[63] O. Taratula et al., Mol. Pharm. 10 (10) (2013) 3946.
[64] M.T. Morgan et al., Cancer Res. 66 (24) (2006) 11913.
[65] Y. Zhang et al., Bioorg. Med. Chem. 19 (8) (2011) 2557.
[66] C. Zhang et al., Polym. Chem. 5 (18) (2014) 5227.
[67] J.J. Khandare et al., Bioconjug. Chem. 17 (6) (2006) 1464.
[68] G.A. Kinberger et al., Tetrahedron 62 (22) (2006) 5280.
[69] B.H. Zinselmeyer et al., Pharm. Res. 19 (7) (2002) 960.
[70] B. Sun et al., Biomacromolecules 13 (10) (2012) 3343.
[71] V.P. Torchilin, J. Control. Release 73 (2–3) (2001) 137.
[72] Y. Lu et al., Nat. Biomed. Eng. 2 (5) (2018) 318.
[73] R. Trivedi, U.B. Kompella, Nanomedicine (Lond) 5 (3) (2010) 485.
[74] Y. Zhang et al., AAPS PharmSciTech 15 (4) (2014) 862.
[75] A. Benahmed et al., Pharm. Res. 18 (3) (2001) 323.
[76] J.E. Chung et al., J. Control. Release 62 (1–2) (1999) 115.
[77] Y. Zhu et al., J. Mater. Chem. B 6 (19) (2018) 3040.
[78] F. Xu et al., ACS Appl. Mater. Interfaces 9 (6) (2017) 5181.
[79] V. Weissig et al., Pharm. Res. 15 (10) (1998) 1552.
[80] H. Cabral et al., J. Control. Release 121 (3) (2007) 146.
[81] M. Murakami et al., Sci. Transl. Med. 3 (64) (2011) 64ra2.
[82] M. Yokoyama et al., Cancer Res. 51 (12) (1991) 3229.
[83] Y. Miura et al., ACS Nano 7 (10) (2013) 8583.
[84] A.C. Anselmo, S. Mitragotri, Bioeng. Transl. Med. 4 (3) (2019) e10143.
[85] C.F. van Nostrum, Soft Matter 7 (7) (2011) 3246.
[86] M. Talelli et al., Nano Today 10 (1) (2015) 93.
[87] S. Matoori, J.-C. Leroux, Mater. Horizons 7 (5) (2020) 1297.
[88] P. Wei et al., J. Control. Release 322 (2020) 81.
[89] D. Shae et al., Nat. Nanotechnol. 14 (3) (2019) 269.
[90] G. Wang et al., Soft Matter 9 (3) (2013) 727.
[91] A. Choucair et al., Langmuir 21 (20) (2005) 9308.
[92] X. Zhang et al., Chem. Soc. Rev. 44 (7) (2015) 1948.
[93] S. Argentiere et al., J. Phys. Chem. B 115 (33) (2011) 16347.
[94] H. Mok et al., Chem. Commun. (Camb.) 48 (69) (2012) 8628.
[95] Y.J. Pan et al., Biomaterials 33 (27) (2012) 6570.
[96] Y. Yuki et al., Mol. Pharm. 18 (4) (2021) 1582.
[97] T. Adachi et al., Materials (Basel) 13 (2020) 19.
[98] Y. Sasaki et al., ACS Biomater. Sci. Eng. 5 (11) (2019) 5752.
[99] Y. Barenholz, J. Control. Release 160 (2) (2012) 117.
[100] A.C. Anselmo, S. Mitragotri, Bioeng. Transl. Med. 1 (1) (2016) 10.
[101] J.L. Fox, Bio/Technology 13 (7) (1995) 635.
[102] R.C. Leonard et al., Breast 18 (4) (2009) 218.
[103] J.A. Silverman, S.R. Deitcher, Cancer Chemother. Pharmacol. 71 (3) (2013) 555.
[104] K. Ando et al., Expert Opin. Pharmacother. 12 (2) (2011) 285.
[105] F.C. Passero Jr et al., Expert Rev. Anticancer Ther. 16 (7) (2016) 697.
[106] L. Belfiore et al., J. Control. Release 277 (2018) 1.
[107] X.L. Song et al., Eur. J. Pharm. Sci. 96 (2017) 129.
[108] N. Shitara et al., Acta Histochem Cytochem 22 (2) (1989) 275.
[109] K.C. Liu et al., Nanomedicine 15 (1) (2019) 285.
[110] Y. Wang et al., J. Mater. Chem. B 7 (7) (2019) 1056.

[111] L. Qin et al., Oncol Lett. 8 (5) (2014) 2000.
[112] L. Sercombe et al., Front. Pharmacol. 6 (2015) 286.
[113] W. Yan et al., Nanomedicine (Lond) 15 (3) (2020) 303.
[114] S.V.K. Rompicharla et al., Chem. Phys. Lipids 208 (2017) 10.
[115] A. Grillone et al., Adv Healthc Mater 4 (11) (2015) 1681.
[116] L. Liu et al., ACS Appl. Mater. Interfaces 9 (8) (2017) 7424.
[117] A. Loureiro et al., Curr. Pharm. Des. 22 (10) (2016) 1371.
[118] G.L. Francis, Cytotechnology 62 (1) (2010) 1.
[119] M. Khoshnejad et al., J. Control. Release 282 (2018) 13.
[120] M. Liang et al., Proc. Natl. Acad. Sci. U S A 111 (41) (2014) 14900.
[121] T. Lin et al., ACS Nano 10 (11) (2016) 9999.
[122] K. Fan et al., ACS Nano 12 (5) (2018) 4105.
[123] C. Gao et al., Acta Pharm. Sin. B 9 (4) (2019) 843.
[124] R. Sleightholm et al., Biomacromolecules 18 (8) (2017) 2247.
[125] S. Guo et al., Nat. Commun. 11 (1) (2020) 972.
[126] S. Li et al., Nat. Biotechnol. 36 (3) (2018) 258.
[127] R. Veneziano et al., Science 352 (6293) (2016) 1534.
[128] P. Guo, Nat. Nanotechnol. 5 (12) (2010) 833.
[129] M.R. Jones et al., Science 347 (6224) (2015) 1260901.
[130] Q. Zhang et al., ACS Nano 8 (7) (2014) 6633.
[131] Z. Ge et al., Small 16 (16) (2020) e1904857.
[132] C.H. Stuart et al., Bioconjug. Chem. 25 (2) (2014) 406.
[133] K.A. Afonin et al., ACS Nano 14 (8) (2020) 9221.
[134] C.M. Hu et al., Proc. Natl. Acad. Sci. U S A 108 (27) (2011) 10980.
[135] Ben-Akiva, E., et al., *Sci. Adv.* (2020) **6** (16), eaay9035
[136] L. Rao et al., ACS Appl. Mater. Interfaces 9 (3) (2017) 2159.
[137] C.M. Hu et al., Nanoscale 5 (7) (2013) 2664.
[138] J. Acosta et al., Curr. Pharm. Des. 10 (2) (2004) 203.
[139] W. Gao et al., Adv. Mater. 25 (26) (2013) 3549.
[140] M. Xuan et al., ACS Appl. Mater. Interfaces 8 (15) (2016) 9610.
[141] T. Okegawa et al., Acta Biochim. Pol. 51 (2) (2004) 445.
[142] L. Zitvogel et al., Nat. Rev. Immunol. 6 (10) (2006) 715.
[143] H. Sun et al., Adv. Mater. 28 (43) (2016) 9581.
[144] C.M. Hu et al., Nature 526 (7571) (2015) 118.
[145] J. Su et al., Adv. Funct. Mater. 26 (8) (2016) 1243.
[146] R.H. Fang et al., Nano Lett. 14 (4) (2014) 2181.
[147] N.E. Toledano Furman et al., Nano Lett. 13 (7) (2013) 3248.
[148] A. Parodi et al., Nat. Nanotechnol. 8 (1) (2013) 61.
[149] L.M. Doyle, M.Z. Wang, Cells 8 (2019) 7.
[150] M.S. Kim et al., Nanomedicine 12 (3) (2016) 655.
[151] Y. Tian et al., Biomaterials 35 (7) (2014) 2383.
[152] A.K. Agrawal et al., Nanomedicine 13 (5) (2017) 1627.
[153] Study Investigating the Ability of Plant Exosomes to Deliver Curcumin to Normal and Colon Cancer Tissue.
[154] Q. Wang et al., Cancer Res. 75 (12) (2015) 2520.
[155] V. Gujrati et al., ACS Nano 8 (2) (2014) 1525.
[156] V. Gujrati et al., Nat. Commun. 10 (1) (2019) 1114.
[157] K. Kuerban et al., Acta Pharm. Sin. B 10 (8) (2020) 1534.
[158] Q. Chen et al., Nano Lett. 20 (1) (2020) 11.
[159] H. Saari et al., J. Control. Release 220 (Pt B) (2015) 727.
[160] H. Qi et al., ACS Nano 10 (3) (2016) 3323.
[161] J. Nam et al., ACS Nano 7 (4) (2013) 3388.
[162] W.H. Chen et al., Biomaterials 34 (34) (2013) 8798.
[163] H. Chen et al., Theranostics 3 (9) (2013) 633.
[164] Y. Liu et al., ACS Nano 10 (2) (2016) 2375.
[165] X. Chen et al., Biomater. Sci. 2 (1) (2014) 121.
[166] J.L. Paris et al., Nanoscale 10 (14) (2018) 6402.
[167] N, V. R., et al., *Nanoscale* (2018) **10** (20), 9616
[168] Z. Li et al., Adv. Funct. Mater. 28 (26) (2018) 1800145.
[169] M. Creixell et al., ACS Nano 5 (9) (2011) 7124.
[170] M. Johannsen et al., Int. J. Hyperthermia 21 (7) (2005) 637.
[171] F. Cengelli et al., ChemMedChem 4 (6) (2009) 988.
[172] L. Wang et al., Biomaterials 34 (1) (2013) 262.
[173] S. Wen et al., Adv. Healthc. Mater. 2 (9) (2013) 1267.
[174] M.A. Lucherelli et al., Angew. Chem. Int. Ed. 59 (33) (2020) 14034.
[175] S.A. Chechetka et al., Angew. Chem. Int. Ed. Engl. 55 (22) (2016) 6476.
[176] Y. Yu et al., ACS Appl. Bio Mater. 2 (8) (2019) 3693.
[177] S.A. Chechetka et al., Nat. Commun. 8 (1) (2017) 15432.
[178] Y. Lu et al., Nat. Commun. 6 (1) (2015) 10066.
[179] H.R. Ali et al., Bioconjug. Chem. 27 (10) (2016) 2486.
[180] L. Scarabelli et al., ACS Nano 8 (6) (2014) 5833.
[181] A. Espinosa et al., Adv. Healthc. Mater. 5 (9) (2016) 1040.
[182] R. Riedel et al., Nanoscale 12 (5) (2020) 3007.
[183] J. Yue et al., Bioconjug. Chem. 28 (6) (2017) 1791.
[184] M.H. Schwenk, Pharmacotherapy 30 (1) (2010) 70.
[185] P. Reimer, T. Balzer, Eur. Radiol. 13 (6) (2003) 1266.
[186] K. Leung, Ferumoxsil. In *Molecular Imaging and Contrast Agent Database (MICAD)*, Bethesda (MD), (2004).
[187] K. Maier-Hauff et al., J. Neurooncol. 103 (2) (2011) 317.
[188] M. Bañobre-López et al., Rep. Pract. Oncol. Radiother. 18 (6) (2013) 397.
[189] L. Feng et al., ACS Nano 12 (11) (2018) 11000.
[190] Hong, X., et al., *Sci. Adv.* (2020) **6** (25), eaaz4462.
[191] J. Li et al., RSC Adv. 8 (43) (2018) 24633.
[192] Z. Liu et al., Nano Res. 2 (2) (2009) 85.
[193] N.W. Kam et al., Proc. Natl. Acad. Sci. U S A 102 (33) (2005) 11600.
[194] J. Lefebvre et al., Nano Lett. 6 (8) (2006) 1603.
[195] A. De la Zerda et al., Nat. Nanotechnol. 3 (9) (2008) 557.
[196] T. Anderson et al., Biomater. Sci. 2 (9) (2014) 1244.
[197] N.W. Kam, H. Dai, J. Am. Chem. Soc. 127 (16) (2005) 6021.
[198] Z. Liu et al., Cancer Res. 68 (16) (2008) 6652.
[199] Z. Liu et al., ACS Nano 1 (1) (2007) 50.
[200] K. Ajima et al., Mol. Pharm. 2 (6) (2005) 475.
[201] K. Ajima et al., J. Phys. Chem. B 110 (39) (2006) 19097.
[202] T. Murakami et al., Mol. Pharm. 3 (4) (2006) 407.
[203] M. Zhang et al., Proc. Natl. Acad. Sci. U S A 105 (39) (2008) 14773.
[204] S.A. Chechetka et al., Chem. Asian J. 10 (1) (2015) 160.
[205] S.A. Chechetka et al., Carbon 97 (2016) 45.
[206] E. Miyako et al., Proc Natl. Acad. Sci. U S A 109 (19) (2012) 7523.
[207] Y. Yu et al., Nat. Commun. 11 (1) (2020) 4117.
[208] J.T. Robinson et al., J. Am. Chem. Soc. 133 (17) (2011) 6825.
[209] Z.M. Markovic et al., Biomaterials 32 (4) (2011) 1121.
[210] S. Wu et al., Int. J. Nanomed. 9 (2014) 1413.
[211] H.S. Jung et al., RSC Adv. 4 (27) (2014) 14197.
[212] D. Ho et al., Sci. Adv. 1 (7) (2015) e1500439.
[213] J. Whitlow et al., J. Control. Release 261 (2017) 62.
[214] E.K. Chow et al., Sci. Transl. Med. 3 (73) (2011) 73ra21.
[215] X. Wang et al., ACS Nano 8 (12) (2014) 12151.
[216] B. Guan et al., Small 6 (14) (2010) 1514.
[217] Y. Yu et al., Nanoscale 10 (19) (2018) 8969.
[218] Y. Yu et al., ACS Appl. Mater. Interfaces 11 (21) (2019) 18978.
[219] Y. Yu et al., Nanoscale Adv 1 (9) (2019) 3406.
[220] X. Sun et al., Nanoscale 11 (6) (2019) 2655.
[221] D. Wang et al., ACS Nano 12 (10) (2018) 10212.
[222] P. Zhu et al., Nano Lett. 19 (3) (2019) 2128.
[223] Y. Yu, E. Miyako, *iScience* (2018) **3**, 134
[224] J. Zhang et al., J. Mater. Chem. B 4 (32) (2016) 5349.
[225] N. Yang et al., Small Methods 4 (9) (2020) 2000147.
[226] J.L. Floyd, E.L. Goodman, JAMA 246 (6) (1981) 675.
[227] M.O. Culjat et al., Acoust. Res. Lett. Online 6 (3) (2005) 125.
[228] S. Wang et al., Adv. Mater. 30 (37) (2018) e1800202.
[229] J. Zhuang et al., ACS Nano 8 (3) (2014) 2812.
[230] P. Horcajada et al., Nat. Mater. 9 (2) (2010) 172.
[231] I.B. Vasconcelos et al., RSC Adv. 2 (25) (2012) 9437.
[232] Q. Chen et al., ACS Appl. Mater. Interfaces 9 (8) (2017) 6712.
[233] K.M. Taylor-Pashow et al., J. Am. Chem. Soc. 131 (40) (2009) 14261.
[234] I. Abanades Lazaro et al., ACS Appl. Mater. Interfaces 10 (6) (2018) 5255.
[235] A.C. McKinlay et al., Chem. Mater. 25 (9) (2013) 1592.
[236] D. Rosenblum et al., Nat. Commun. 9 (1) (2018) 1410.
[237] M.V. Liberti, J.W. Locasale, Trends Biochem. Sci. 41 (3) (2016) 211.
[238] N. Deirram et al., Macromol. Rapid Commun. 40 (10) (2019) e1800917.
[239] M.P. Gamcsik et al., Biomarkers 17 (8) (2012) 671.
[240] Y. Li et al., Biomaterials 32 (27) (2011) 6633.
[241] S.Y. Lee et al., Biomaterials 34 (2) (2013) 552.
[242] E. Gobin et al., BMC Cancer 19 (1) (2019) 581.
[243] N. Aggarwal, B.F. Sloane, Proteomics Clin. Appl. 8 (5–6) (2014) 427.
[244] M. Li et al., Front. Chem. 8 (2020) 647.
[245] H. Chen et al., Biomater. Sci. 2 (7) (2014) 996.
[246] A.R. Rastinehad et al., Proc. Natl. Acad. Sci. U S A 116 (37) (2019) 18590.
[247] A.C. Del Valle et al., Biomater. Sci. 8 (7) (2020) 1934.
[248] X. Huang, M.A. El-Sayed, Alexandria J. Med. 47 (1) (2011) 1.
[249] J. Xi et al., ACS Biomater. Sci. Eng. 4 (3) (2018) 1083.
[250] P. Nonsuwan, K. Matsumura, ACS Appl. Polym. Mater. 1 (2) (2019) 286.
[251] A. Hervault, N.T. Thanh, Nanoscale 6 (20) (2014) 11553.
[252] P. Kheirkhah et al., Sci. Rep. 8 (1) (2018) 11417.
[253] S. Sánchez-Cabezas et al., Dalton Trans. 48 (12) (2019) 3883.
[254] K. Hayashi et al., ACS Biomater. Sci. Eng. 3 (1) (2017) 95.

[255] S. Mullick Chowdhury et al., Ultrasonography 36 (3) (2017) 171.
[256] A. Schroeder et al., Langmuir 23 (7) (2007) 4019.
[257] A.R. Salgarella et al., Sci. Rep. 8 (1) (2018) 9893.
[258] P. Tharkar et al., Front. Bioeng. Biotechnol. 7 (2019) 324.
[259] C. Yuan et al., Nat. Rev. Chem. 3 (10) (2019) 567.
[260] S. Li et al., Chem. Sci. 11 (33) (2020) 8644.
[261] R. Chang, X. Yan, Small Struct. 1 (2) (2020) 2000068.
[262] A. Mandal et al., Sci. Transl. Med. 10 (2018) 467.
[263] D.S. Chen, I. Mellman, Immunity 39 (1) (2013) 1.
[264] S. Ahmed, K.R. Rai, Best Pract. Res. Clin. Haematol. 16 (1) (2003) 69.
[265] S. Menon et al., Cancers (Basel) 8 (2016) 12.
[266] S.B. Stephan et al., Nat. Biotechnol. 33 (1) (2015) 97.
[267] R.S. Riley et al., Nat. Rev. Drug Discov. 18 (3) (2019) 175.
[268] C. Lai et al., Theranostics 8 (6) (2018) 1723.
[269] E. Yuba et al., Biomaterials 67 (2015) 214.
[270] L. Liu et al., Mol. Ther. 26 (1) (2018) 45.
[271] M. Huo et al., J. Control. Release 245 (2017) 81.
[272] Y. Lu et al., Mol. Ther. 24 (2) (2016) 364.
[273] H. Li et al., Theranostics 7 (18) (2017) 4383.
[274] Y. Tao et al., Biomaterials 35 (37) (2014) 9963.
[275] K. Cheng et al., Nano Lett. 18 (5) (2018) 3250.
[276] A.K. Kosmides et al., Biomaterials 118 (2017) 16.
[277] K. Ueda et al., Acta Biomater. 29 (2016) 103.
[278] O.A. Ali et al., Nat. Mater. 8 (2) (2009) 151.
[279] M. Zhu et al., J. Control. Release 272 (2018) 72.
[280] J. Kim et al., Nat. Biotechnol. 33 (1) (2015) 64.
[281] A. Ruiz-de-Angulo et al., ACS Nano 10 (1) (2016) 1602.
[282] H. Jin et al., Theranostics 6 (11) (2016) 2000.
[283] C. Wang et al., Nano Lett. 16 (4) (2016) 2334.
[284] Y. Ye et al., ACS Nano 10 (9) (2016) 8956.
[285] L. Guo et al., ACS Nano 8 (6) (2014) 5670.
[286] L. Wu et al., Nat. Rev. Chem. 5 (6) (2021) 406.
[287] C. Zhang et al., Nat. Commun. 12 (1) (2021) 2934.
[288] Y. Jiang et al., Nat. Commun. 12 (1) (2021) 742.
[289] C. Zhang, K. Pu, Chem. Soc. Rev. 49 (13) (2020) 4234.
[290] Y. Zhang et al., Adv. Mater. 32 (34) (2020) e2002661.
[291] S. Li et al., Adv. Mater. 33 (21) (2021) e2100595.
[292] L. Li et al., Theranostics 8 (3) (2018) 860.
[293] L. Luo et al., J. Control. Release 278 (2018) 87.
[294] H.L. Hauksdottir, T.J. Webster, J. Biomed. Nanotechnol. 14 (3) (2018) 510.
[295] M.J. Lind, Medicine 36 (1) (2008) 19.
[296] K. Lohner, S.E. Blondelle, Comb. Chem. High Throughput Screen 8 (3) (2005) 241.
[297] H. Sun et al., J. Control. Release 290 (2018) 11.
[298] W. Tang, M.L. Becker, Chem. Soc. Rev. 43 (20) (2014) 7013.
[299] A. Komin et al., Adv. Drug Deliv. Rev. 110–111 (2017) 52.
[300] J. Zhao et al., J. Mater. Chem. B 5 (40) (2017) 8035.
[301] W.C. Wimley, ACS Chem. Biol. 5 (10) (2010) 905.
[302] C. Leuschner, W. Hansel, Curr. Pharm. Des. 10 (19) (2004) 2299.
[303] S.F. Sui et al., J. Biochem. 116 (3) (1994) 482.
[304] B. Bechinger, Biochim. Biophys .Acta 1462 (1–2) (1999) 157.
[305] H.W. Huang, Biochemistry 39 (29) (2000) 8347.
[306] I.R. Mellor, M.S. Sansom, Proc. R. Soc. Lond. B Biol. Sci. 239 (1296) (1990) 383.
[307] E.L. Merrifield et al., Int. J. Pept. Protein Res. 46 (3–4) (1995) 214.
[308] S.J. Ludtke et al., Biochim. Biophys. Acta 1190 (1) (1994) 181.
[309] Y. Pouny et al., Biochemistry 31 (49) (1992) 12416.
[310] J. Dufourcq et al., Biochim. Biophys. Acta 859 (1) (1986) 33.
[311] C.E. Dempsey, B. Sternberg, Biochim. Biophys. Acta (BBA) - Biomembranes 1061 (2) (1991) 175.
[312] J.P. Segrest et al., Adv. Protein Chem. 45 (1994) 303.
[313] M. Roux et al., Biochemistry 33 (1) (1994) 307.
[314] R.A. Cruciani et al., Proc. Natl. Acad. Sci. U S A 88 (9) (1991) 3792.
[315] Y. Ohsaki et al., Cancer Res. 52 (13) (1992) 3534.
[316] M.A. Baker et al., Cancer Res. 53 (13) (1993) 3052.
[317] P.W. Soballe et al., Int. J. Cancer 60 (2) (1995) 280.
[318] H. van Zoggel et al., Amino Acids 42 (1) (2012) 385.
[319] H. van Zoggel et al., PLoS ONE 7 (9) (2012) e44351.
[320] K.R. Wang et al., Peptides 29 (6) (2008) 963.
[321] A.J. Moore et al., Pept. Res. 7 (5) (1994) 265.
[322] A. Risso et al., Cell. Immunol. 189 (2) (1998) 107.
[323] B. Skerlavaj et al., J. Biol. Chem. 271 (45) (1996) 28375.
[324] A. Risso et al., Mol. Cell. Biol. 22 (6) (2002) 1926.
[325] M.-X. Meng et al., J. Huazhong Univ. Sci. Technolog. Med. Sci. 34 (4) (2014) 529.
[326] S. Kim et al., Peptides 24 (7) (2003) 945.
[327] L. Meng et al., Oncol. Lett. 13 (1) (2017) 511.
[328] R. Beesoo et al., Mutat. Res. 768 (2014) 84.
[329] P. Saharinen et al., Trends Mol. Med. 17 (7) (2011) 347.
[330] Z.F. Yi et al., Int. J. Cancer 124 (4) (2009) 843.
[331] J.P. Jang et al., PLoS ONE 12 (9) (2017) e0184339.
[332] S.A. Rosenberg et al., Nat. Med. 10 (9) (2004) 909.
[333] Y. Zhang et al., Nutr. Cancer 66 (8) (2014) 1371.
[334] X. Li et al., Cancer Biol. Ther. 16 (3) (2015) 450.
[335] G. Gakhar et al., Anticancer Res. 34 (8) (2014) 3981.
[336] L. Meurling et al., Int. J. Oncol. 35 (2) (2009) 281.
[337] N.H. Park et al., J. Am. Chem. Soc. 140 (12) (2018) 4244.
[338] G. Zhong et al., Biomaterials 199 (2019) 76.
[339] H. Takahashi et al., Sci. Rep. 9 (1) (2019) 1096.
[340] N. Papo, Y. Shai, Cell. Mol. Life Sci. 62 (7–8) (2005) 784.
[341] S. Riedl et al., Chem. Phys. Lipids 164 (8) (2011) 766.
[342] A.T.Y. Yeung et al., Cell. Mol. Life Sci. 68 (13) (2011) 2161.
[343] A. Chrzanowska et al., Eur. J. Med. Chem. 185 (2020) 111810.
[344] B.A. Lipsky, C.A. Baker, Clin. Infect. Dis. 28 (2) (1999) 352.
[345] U. Galm et al., Chem. Rev. 105 (2) (2005) 739.
[346] I.S. Haslam et al., Drug Metab. Dispos. 39 (12) (2011) 2321.
[347] Y. Zheng, et al., *Biomater. Sci.* (2021).
[348] S. Zhou et al., Chem. Commun. (Camb.) 55 (59) (2019) 8615.
[349] N.S. Forbes, Nat. Rev. Cancer 10 (11) (2010) 785.
[350] W.B. Coley, Clin. Orthop. Relat. Res. 262 (1991) 3.
[351] W.B. Coley, *Proc R Soc Med* (1910) **3** (Surg Sect), 1.
[352] J.M. Brown, W.R. Wilson, Nat. Rev. Cancer 4 (6) (2004) 437.
[353] L.H. Dang et al., Proc. Natl. Acad. Sci. U S A 98 (26) (2001) 15155.
[354] G. Chen et al., Cancer Sci. 100 (12) (2009) 2437.
[355] C. Nagakura et al., Anticancer Res. 29 (6) (2009) 1873.
[356] K.B. Low et al., Nat. Biotechnol. 17 (1) (1999) 37.
[357] S.H. Kim et al., Cancer Res. 69 (14) (2009) 5860.
[358] J.F. Toso et al., J. Clin. Oncol. 20 (1) (2002) 142.
[359] D.M. Heimann, S.A. Rosenberg, J. Immunother. 26 (2) (2003) 179.
[360] J. Nemunaitis et al., Cancer Gene Ther. 10 (10) (2003) 737.
[361] D.-W. Zheng et al., Nat. Commun. 9 (1) (2018) 1680.
[362] F. Chen et al., Biomaterials 214 (2019) 119226.
[363] X. Yang et al., Nano Today 37 (2021) 101100.
[364] O. Felfoul et al., Nat. Nanotechnol. 11 (11) (2016) 941.
[365] D. Kuzajewska et al., Biology (Basel) 9 (2020) 5.
[366] I.S. Khalil et al., Annu. Int. Conf. IEEE Eng. Med. Biol. Soc. 2013 (2013) 5299.
[367] D. Gandia et al., Small 15 (41) (2019) e1902626.
[368] P.E. Georghiou et al., Mutat. Res. Lett. 225 (1) (1989) 33.
[369] W. Chen et al., ACS Nano 12 (6) (2018) 5995.
[370] C.H. Luo et al., Nano Lett. 16 (6) (2016) 3493.
[371] L. Liu et al., Adv. Funct. Mater. 30 (10) (2020) 1910176.
[372] M. Huo et al., Angew. Chem. Int. Ed. Engl. 59 (5) (2020) 1906.
[373] Y. Wang et al., J. Control. Release 280 (2018) 39.
[374] S. Suh et al., Adv Sci (Weinh) 6 (3) (2019) 1801309.
[375] Q. Hu et al., Nano Lett. 15 (4) (2015) 2732.
[376] N.E. Sharpless, R.A. Depinho, Nat. Rev. Drug Discov. 5 (9) (2006) 741.
[377] J. Gonzalez-Valdivieso et al., Int. J. Pharm. 599 (2021) 120438.
[378] S. Hua et al., Front. Pharmacol. 9 (2018) 790.

Nishant Kumar received his Master's degree as a dual degree graduate between the Japan Advanced Institute of Science and Technology (JAIST), and the University of Delhi, India. During his Master's he investigated ring-opening metathesis polymers and their uses in various biomedical applications. Currently, he is pursuing his Ph. D. in the field of anticancer therapy with Prof. Kazuaki Matsumura at the School of Materials Science, JAIST. His research interests include polymerization reactions and the organic synthesis of new biomolecules and evaluating their bioactivity.

Sajid Fazal received his Ph.D. from the Center for Nanoscience and Molecular Medicine, Amrita Institute of Medical Science (Kerala, India) where he worked on the use of inorganic nanoparticles such as gold and iron oxide nanoparticles for cancer theranostic applications, including photothermal therapy, radiofrequency hyperthermia, and magnetic resonance imaging. He is presently working as a postdoctoral research associate at JAIST.

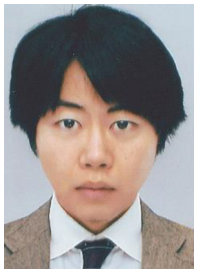

Eijiro Miyako received his Ph.D. from Kyushu University, Japan. During his Ph.D. thesis, he worked for a year as a research fellow of the Japan Society for the Promotion of Science. Shortly thereafter, he joined the National Institute of Advanced Industrial Science and Technology as an independent researcher. He was also a visiting scientist at the Centre National de la Recherche Scientifique (France) and Nanyang Technological University (Singapore). He is currently an associate professor at the School of Materials Science, JAIST. His interests include interdisciplinary research in bioengineering, materials chemistry, nanotechnology, and nanomedicine.

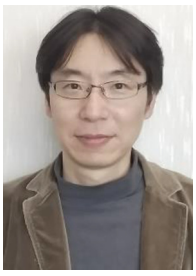

Kazuaki Matsumura is a professor at JAIST. He received his Ph.D. from Kyoto University in the field of polymer chemistry in 2004. He moved to JAIST in 2011 to set up a biomaterials laboratory and continues to investigate polymeric biomaterials and biomedical engineering applications for polymers. His research interests include the molecular design of protective materials for biomolecules and cells, drug delivery system carriers, and tissue engineering materials.

Robin Rajan received his Ph.D. from JAIST in 2016 in materials science. He also completed his first postdoctoral study at JAIST and then moved to Nanyang Technological University (Singapore) for another postdoctoral tenure. He later returned to JAIST, where he has been working since 2018 as an assistant professor. His research interests include polymer chemistry, organic synthesis, and biomaterials, with a focus on the effects that polymers have on cells, proteins, and other biologically relevant molecules.